

RESEARCH

Open Access



# Targeted activation of ErbB4 receptor ameliorates neuronal deficits and neuroinflammation in a food-borne polystyrene microplastic exposed mouse model

Chong Liu<sup>1†</sup>, Yan Zhao<sup>2†</sup>, Wei Zhang<sup>1,3</sup>, Ji-Ji Dao<sup>1</sup>, Qian Li<sup>1</sup>, Jia Huang<sup>2</sup>, Zhen-Feng Li<sup>4</sup>, Yu-Ke Ma<sup>5</sup>, Chen-Meng Qiao<sup>6</sup>, Chun Cui<sup>6</sup>, Shuang-Xi Chen<sup>7</sup>, Li Yu<sup>2</sup>, Yan-Qin Shen<sup>6</sup> and Wei-Jiang Zhao<sup>1,8\*</sup>

## Abstract

The impact of polystyrene microplastics (PS-MPs) on the nervous system has been documented in the literature. Numerous studies have demonstrated that the activation of the epidermal growth factor receptor 4 (ErbB4) is crucial in neuronal injury and regeneration processes. This study investigated the role of targeted activation of ErbB4 receptor through a small molecule agonist, 4-bromo-1-hydroxy-2-naphthoic acid (C11H7BrO3, E4A), in mitigating PS-MPs-induced neuronal injury. The findings revealed that targeted activation of ErbB4 receptor significantly ameliorated cognitive behavioral deficits in mice exposed to PS-MPs. Furthermore, E4A treatment upregulated the expression of dedicator of cytokinesis 3 (DOCK3) and Sirtuin 3 (SIRT3) and mitigated mitochondrial and synaptic dysfunction within the hippocampus of PS-MPs-exposed mice. E4A also diminished the activation of the TLR4-NF-κB-NLRP3 signaling pathway, consequently reducing neuroinflammation. In vitro experiments demonstrated that E4A partially alleviated PS-MPs-induced hippocampal neuronal injury and its effects on microglial inflammation. In conclusion, the findings of this study indicate that targeted activation of ErbB4 receptor may mitigate neuronal damage and subsequent neuroinflammation, thereby alleviating hippocampal neuronal injury induced by PS-MPs exposure and ameliorating cognitive dysfunction. These results offer valuable insights for the development of potential therapeutic strategies.

**Keywords** PS-MPs, Neuronal damage, Neuroinflammation, ErbB4 receptor, Small molecule, Mitochondrial damage, Cognitive dysfunction

<sup>†</sup>Chong Liu and Yan Zhao contributed equally to this work as co-first authors.

\*Correspondence:  
Wei-Jiang Zhao  
weijiangzhao@jiangnan.edu.cn

Full list of author information is available at the end of the article



© The Author(s) 2025. **Open Access** This article is licensed under a Creative Commons Attribution-NonCommercial-NoDerivatives 4.0 International License, which permits any non-commercial use, sharing, distribution and reproduction in any medium or format, as long as you give appropriate credit to the original author(s) and the source, provide a link to the Creative Commons licence, and indicate if you modified the licensed material. You do not have permission under this licence to share adapted material derived from this article or parts of it. The images or other third party material in this article are included in the article's Creative Commons licence, unless indicated otherwise in a credit line to the material. If material is not included in the article's Creative Commons licence and your intended use is not permitted by statutory regulation or exceeds the permitted use, you will need to obtain permission directly from the copyright holder. To view a copy of this licence, visit <http://creativecommons.org/licenses/by-nc-nd/4.0/>.

## Introduction

Microplastics (MPs), defined as plastic particles, films, and fibers with diameters less than 5 mm, persist in the environment for extended periods. Their annual emissions have risen markedly, thereby increasing the likelihood of human exposure [1]. While the significant environmental impact of plastic waste has garnered substantial attention from scientists, policymakers, and the general public, the implications of plastic contamination in food and beverages on human health remain largely unexplored.

Ingestion is recognized as the primary pathway for human exposure to MPs [2], with the ocean serving as a significant reservoir of microplastic pollution. MPs may progressively accumulate within marine organisms across successive trophic levels, concomitant with the advancement of trophic hierarchies and the growth and development of marine life. This accumulation results in increasingly elevated concentrations, ultimately leading to human consumption and the potential deleterious accumulation of MPs in vital tissues and organs, such as the intestines, liver, kidneys, and brain, as apex predators [3–5]. Consequently, it is imperative to examine the health risks posed by MPs as an emerging contaminant in the food supply.

Numerous studies have demonstrated that MPs can traverse the blood-brain barrier (BBB) and infiltrate brain tissue, thereby disrupting the normal growth and development of neural cells, inducing histopathological damage to the brain, and consequently exerting neurotoxic effects [6, 7]. The hippocampus, a critical brain region associated with cognitive functions such as learning and memory, is particularly susceptible to these effects [8, 9]. Exposure to MPs has been shown to impair hippocampal-dependent learning and memory functions, thus accelerating memory decline in aging mice [9, 10]. Neuronal damage results in diminished synaptic plasticity, leading to a decline in cognitive function. In mice, MPs ingestion exacerbates neuronal damage and impairs synaptic plasticity [9]. Neurons can affect glial cell growth and function, and studies suggest that neuronal injury may trigger microglial inflammation [11, 12]. Currently, the potential effects of MPs on cognitive impairment remain uncertain, necessitating further investigation into the mechanisms by which MPs exposure may contribute to cognitive deficits, to inform potential clinical interventions.

The preservation of synaptic efficacy and the prevention of neuronal degeneration are contingent upon the stabilization of mitochondrial function, the impairment of which may result in diminished synaptic performance [13, 14]. Mitochondria are integral to cognitive processes through their regulation of synaptic function. Recent studies suggest that polystyrene (PS)-MPs compromise

gastric cell viability, increase the production of reactive oxygen species (ROS), trigger apoptosis through mitochondria-dependent pathways, and disturb mitochondrial kinetic homeostasis [15]. Nonetheless, additional research is necessary to comprehensively elucidate these mechanisms.

Epidermal growth factor receptor 4 (ErbB4) serves as a crucial receptor facilitating the physiological functions of Neuregulin 1 (NRG1) and is prominently expressed in several critical brain regions of adult animals, notably the hippocampus [16]. Dysfunction of NRG1/ErbB4 signaling in the hippocampus might mediate long-term memory decline after systemic inflammation [17], suggesting that the abnormality of ErbB4 receptor might be related to the decline of memory ability. Recent studies have found that the ErbB4-postsynaptic density 95 (PSD95) binding induced by the physiological activities of neurons can promote the formation of excitatory synapses of ErbB4-positive interneurons, indicating that ErbB4 plays an important role in the regulation of synaptic function [18]. In addition, ErbB4 exists in mitochondria, and the loss of mitochondrial membrane potential is accompanied by a decrease in ErbB4 expression, suggesting that ErbB4 is involved in the regulation of mitochondrial function [19]. ErbB4 has been implicated in regulating synaptic plasticity [20] and cell survival through a mitochondria-dependent mechanism [19]. Nevertheless, the potential impact of MPs on neuronal synaptic dysfunction in conjunction with mitochondrial damage, and the role of ErbB4 in this process, remain uncertain.

Activation of ErbB4 receptor has the potential to enhance synaptic function, thereby offering a therapeutic approach for cognitive impairments [21–23]. While recombinant Neuregulins (rNRGs) protein therapy can effectively target and activate the ErbB4 receptor [24], its clinical application is considerably constrained by high treatment costs and a limited half-life [25]. In addition to ErbB4, NRG1 may activate ErbB3 receptor in cells overexpressing ErbB2 receptor, thereby promoting the formation of ErbB3/ErbB2 complexes, thus inducing or accelerating cancer progression [25]. Conversely, small molecule compounds acting as agonists present a promising alternative to overcome these limitations [26]. In this context, our previous research utilized molecular docking technology to screen and identify a small molecule compound, 4-bromo-1-hydroxy-2-naphthoic acid (C11H7BrO3, E4A), capable of activating ErbB4 receptor and preventing neuronal senescence induced by D-Galactose through inhibition of the ferroptosis pathway [27]. Nonetheless, the precise mechanism by which ErbB4 receptor activation mediates cognitive function improvement in the context of PS-MPs exposure remains to be elucidated.

We hypothesized that targeted activation of ErbB4 receptor could improve mitochondrial function and inhibit synaptic damage, thereby reversing the cognitive behavioral deficits caused by PS-MPs exposure. By administering the small molecule ErbB4 receptor agonist to PS-MPs-exposed mice, we found that targeted activation of ErbB4 receptor could inhibit neuronal synaptic damage and subsequent neuroinflammation. This approach offers a potential therapeutic strategy for addressing cognitive impairments induced by PS-MPs exposure, providing a reference for the prevention and treatment of central nervous system damage potentially associated with food-borne PS-MPs exposure.

## Materials and methods

### Animals and drug administration

Animal experiments were conducted at the Animal Experimental Center of Wuxi School of Medicine, Jiangnan University, following approval from the Animal Experimentation Ethics Committee of Jiangnan University and in accordance with the general regulations of the National Institutes of Health (approval code: JN. No. 20230228t0320515).

Thirty-two male C57BL/6 mice, aged six months, were obtained from Changzhou Cavens Laboratory Animal Co., Ltd. Prior to the initiation of the study, the mice underwent a one-week acclimatization period in a specific pathogen-free (SPF) environment, maintained at a temperature of 25 °C with a 12-hour light/dark cycle. During this period, the mice had ad libitum access to food and water. Post-acclimatization, the mice were randomly allocated into four groups ( $n = 8$  per group): a control group, a C11H7BrO<sub>3</sub> (E4A) group, a PS-MPs group, and a PS-MPs + C11H7BrO<sub>3</sub> treatment group.

In light of the substantial consumption rates of fruits and vegetables, PS-MPs with an average diameter of approximately 2  $\mu\text{m}$  [28, 29], representing the average size found in these food items, were chosen as the exposure material for this study. Ingestion is recognized as the primary route of human exposure to PS-MPs; therefore, oral gavage was employed as the method of administration. Following the acclimatization period, the experimental protocol commenced. Initially, during the two weeks preceding the experiment, both the PS-MPs group and the PS-MPs + C11H7BrO<sub>3</sub> group were administered PS-MPs by gavage at a dosage of 50 mg/kg body weight every two days. Meanwhile, the control group and the C11H7BrO<sub>3</sub> group were administered an equivalent volume of 0.1 M phosphate-buffered saline via gavage. During the third and fourth weeks, the mice in each experimental group continued to receive the same gavage treatment as administered in the preceding two weeks. Concurrently, mice in the C11H7BrO<sub>3</sub> group and the PS-MPs + C11H7BrO<sub>3</sub> group were additionally subjected to

daily intraperitoneal injections of C11H7BrO<sub>3</sub> at a dosage of 400 ng/kg body weight over a two-week period. Mice in both the control and PS-MPs groups received an equivalent volume of 0.1 M PBS via intraperitoneal injection.

The dosage and frequency of PS-MPs gavage were determined in accordance with existing studies on PS-MPs [2, 5, 30–36]. Based on the estimated daily intake of MPs in humans, which ranges from 0.23 to 11.52 mg/kg for an average body weight of approximately 62 kg [5, 30], the equivalent dose for mice was calculated using the standard pharmacological and toxicological formula: equivalent dose (mg/kg BW) for mice = human dose (mg/kg BW)  $\times$  Km ratio, where the Km ratio is 12.3 [31]. Consequently, the equivalent dose for mice is estimated to range from 2.83 to 141.70 mg/kg. For C57BL/6 mice with an average body weight of approximately 0.03 kg, the calculated dose is approximately 0.085 to 4.25 mg/day. In consideration of the concentrations and durations reported in previous studies [2, 32–36], a moderate dose of 1.5 mg/day was chosen from within the specified range. Consequently, the administration concentration for mice was determined to be approximately 50 mg/kg. A regimen of administration every other day was implemented over a 4-week period for the animal experiment.

Upon the completion of the exposure and drug administration phase, an 11-day behavioral experiment was conducted. This experiment included one day of open field testing, two days dedicated to novel object recognition (NOR) testing, one day of Y-maze testing, and seven days of water maze testing. Immediately following the conclusion of the behavioral assessments, the mice were anesthetized, and brain tissues were collected for further analysis.

### Behavioral assays

The mice were allowed a minimum acclimation period of 30 min in the experimental environment prior to testing. Initially, less demanding behavioral assessments were conducted, followed by more challenging evaluations, adhering to the test sequence outlined in previous reports [37–39].

#### The open field experiment

The open field experiment is employed to assess anxiety and depression in mice. Mice were permitted to freely explore a test field measuring 50  $\times$  50 cm<sup>2</sup> for a duration of 5 min, during which their exploration trajectories and behavioral parameters were recorded using a video tracking system.

#### The new object recognition experiment

The novel object recognition (NOR) experiment is utilized to evaluate learning and memory. During the

familiarization phase, two identical cylindrical blocks were placed on opposite sides of the experimental apparatus, each positioned 5 cm from the corners of the enclosure. Mice were given 5 min to freely explore the blocks and their surroundings. Twenty-four hours later, one of the cylindrical blocks was replaced with a conical object, and a video tracking system was used to document the mice's exploration patterns and behavioral responses during the subsequent 5-min period.

#### **The Y-maze experiment**

The Y-maze experiment serves as a method for evaluating spatial recognition memory abilities. In this procedure, a baffle is employed to obstruct the starting arm of the maze, and mice are positioned facing the wall from the starting arm. The mice are then allowed to explore the Y-maze freely for a duration of 5 min. After an interval of 1 h, the mice are again permitted to explore the arms freely for another 5 min, during which the frequency of consecutive entries into the three arms in an alternating pattern is recorded.

#### **The Morris water maze**

The Morris water maze (MWM) is an experimental paradigm designed to assess hippocampal dependency and long-term spatial memory. During the training phase, mice undergo four trials per day in the MWM from days 1 to 6, with each trial involving placement into different quadrants of water while facing the wall. On day 7, a probe trial is conducted to evaluate memory consolidation, wherein the mice are given 60 s to swim freely. The frequency of crossings over the previous platform location by each mouse and the proportion of time spent exploring the relevant quadrant are systematically observed and documented.

#### **Cell processing**

The HT22 mouse hippocampal neuron cell line and the BV2 mouse microglia cell line were obtained from Procell Life Science & Technology Co., Ltd. (catalog numbers CL-0493 A and CL-0697, respectively) and were cultured in high glucose DMEM medium at 37 °C with 5% CO<sub>2</sub>.

#### **C11H7BrO3 treatment of a hippocampal neuron cell damage model induced by PS-MPs**

The investigation focused on assessing the reparative effects of C11H7BrO3 on PS-MPs injury *in vitro*, as well as elucidating the underlying mechanisms, utilizing HT22 hippocampal neurons model induced by PS-MPs. The neuronal cells were allocated into four groups: a control group, a C11H7BrO3-treated group, a PS-MPs group, and a combined PS-MPs + C11H7BrO3 treatment group. The control group was treated with vehicle, the C11H7BrO3 group was treated with 10 nM C11H7BrO3

for 24 h, PS-MPs group was damaged with 100 µg/mL PS-MPs for 24 h, and the PS-MPs + C11H7BrO3 group was initially treated with 100 µg/mL PS-MPs for 24 h, followed by treatment with 10 nM C11H7BrO3 for additional 24 h. The effect of C11H7BrO3 on the alteration of ErbB4 signaling pathway and the repair of mitochondrion-related signaling damage in HT22 cells under PS-MPs was studied. Furthermore, BV2 cells were treated with conditioned media from each of the aforementioned groups to evaluate the impact of neuronal treatment on microglial activation by assessing the expression of inflammatory factors.

#### **Golgi staining and analysis**

The Golgi-Cox staining procedure was conducted utilizing the FD Rapid GolgiStain™ Kit (BA1808, Saint-Bio, Shanghai, China). In summary, the brains of the mice were submerged in the Golgi-Cox solution for a duration of 14 days. Serial coronal sections, each with a thickness of 100 µm, were then prepared, stained with the working solution, and subsequently coverslipped. To evaluate the density of dendritic spines and mushroom spines within the hippocampal regions of cornu ammonis 1 (CA1), CA3, and the dentate gyrus (DG), the number of spinous processes was quantified along randomly selected dendritic segments, each measuring 10 µm in length. The density of dendritic spines and mushroom spines was determined by dividing the total number of spinous processes by the length of the dendritic segment.

#### **Tissue immunofluorescence staining**

Following perfusion, the brains were extracted and sequentially immersed in sucrose solutions of increasing concentrations (20%, 25%, and 30%) and subsequently stored at 4 °C. The brains were then embedded in Tissue Tek O.C.T. compound (4583, Sakura Finetek, USA) and sectioned into serial coronal slices with a thickness of 8 µm for immunofluorescence staining. After being washed three times with PBS, the tissue sections underwent antigen retrieval for 60 min in a citrate antigen retrieval solution (pH 6.0) at 99 °C. Subsequently, a blocking step was performed using 10% goat serum, after which the tissue sections were incubated overnight at room temperature with a primary antibody mixture. Specifically, the sections were treated with a mouse anti-β3-tubulin antibody (1:100, sc80016, Santa Cruz Biotechnology, USA) in combination with one of the following antibodies: rabbit anti-p-ErbB4 antibody (1:200, bs-3220R, Bioss, Beijing, China), and rabbit anti-synaptophysin (SYP) antibody (1:200, AF8091, Beyotime, Shanghai, China). Additionally, the sections were incubated with rabbit anti-ionized calcium-binding adapter molecule 1 (IBA1) antibody (1:100, bs-1363R, Bioss, Beijing, China) and rabbit anti-glial fibrillary acidic protein



(GFAP) antibody (1:200, BA0056, Boster, Wuhan, China). After three washes with PBS (5 min each), the tissue sections were incubated for additional 2 h with a mixture of Alexa Fluor 488-conjugated goat anti-mouse IgG (1:200, BA1126, Boster, Wuhan, China) and Alexa Fluor 594-conjugated goat anti-rabbit IgG (1:200, BA1142, Boster, Wuhan, China). Subsequently, the samples were mounted with an anti-fade mounting solution containing DAPI (P0131, Beyotime, Shanghai, China). Fluorescence images were acquired using a fluorescence microscope (Axio Imager Z2, Carl Zeiss AG, Germany).

### Western blot analysis

Total proteins were extracted from HT22 and BV2 cells, as well as from mouse hippocampal tissues. The proteins were separated by 4–12% sodium dodecyl sulfate polyacrylamide gel electrophoresis (SDS-PAGE) (F15412MGel, ACE, Changzhou, China), transferred onto a polyvinylidene fluoride (PVDF) membrane (FFP39, Merck Millipore Ltd, Darmstadt, Germany), and blocked with 3% bovine serum albumin (BSA) at room temperature for one hour. This was followed by an overnight incubation with primary antibodies at 4 °C, as detailed in Table S1. The membrane underwent three washes with Tris-buffered saline with 0.05% Tween 20 (TBST), each lasting 10 min. It was then incubated with a horseradish peroxidase (HRP)-conjugated secondary antibody at a dilution of 1:2000 (A0192, A0208, Beyotime, Shanghai, China) at room temperature for one hour. Protein bands were visualized utilizing an enhanced chemiluminescence (ECL) detection system (JS-M6P, Peiqing, Shanghai, China), and the band densities were quantified using ImageJ software (version 1.6.0, NIH, Bethesda, MA, USA).

### Transmission electron microscopy (TEM) analysis

The mouse hippocampal tissue was sectioned into 1 mm<sup>3</sup> cubes and subjected to fixation in a 2.5% glutaraldehyde solution at 4 °C for 24 h in the absence of light. Subsequently, the samples underwent treatment with a 5% osmium tetroxide solution for approximately 1.5 h. Following staining with uranyl acetate and lead citrate, ultrathin sections measuring 50–70 nm in thickness were rinsed with deionized water and examined using a transmission electron microscope (HT7700, Hitachi, Tokyo, Japan). From each sample, three non-consecutive slices were selected for microscopic imaging, with an interval exceeding 50 µm between slices. A minimum of 20 images from different fields of view per slice were captured for statistical analysis. Quantitative analysis of synaptic parameters, including synapse count, synaptic cleft width, postsynaptic density thickness, and synaptic active zone length [40], was performed using ImageJ software (version 1.6.0, NIH, Bethesda, MD, USA). Mitochondrial

damage was characterized based on morphological features, with criteria for severely compromised mitochondria encompassing extensive fragmentation or dissolution of mitochondrial cristae, pronounced rupture of the outer membrane, and vacuolization [41–44]. ImageJ software (version 1.6.0, NIH, Bethesda, MA, USA) was employed to quantitatively assess mitochondrial damage indicators per unit area.

### Evaluation of oxidative stress in hippocampal neurons in vitro

The protein concentration of HT22 hippocampal neurons was measured by BCA method (BK0001-01, BOYI, Changzhou, China). The levels of total superoxide dismutase (T-SOD, A001-1-2, Jiancheng, Nanjing, China), glutathione (GSH, A006-2-1, Jiancheng, Nanjing, China), glutathione peroxidase (GSH-Px, A005-1-2, Jiancheng, Nanjing, China) and malondialdehyde (MDA, A003-1-2, Jiancheng, Nanjing, China) were measured using a commercial kit as instructed by the supplier. Their concentrations were measured by OD values using a microplate reader (Synergy H4, Bio-Tek, USA).

### Quantification of adenosine triphosphate (ATP) levels in cultured hippocampal neurons

The protein extract from HT22 hippocampal neurons was prepared for analysis. ATP levels were quantified utilizing a commercially available assay kit (A095-1-2, Jiancheng, Nanjing, China). The concentration of ATP was determined by measuring the optical density (OD) value using a microplate reader (Synergy H4, Bio-Tek, USA).

### Cell immunofluorescence staining

Hippocampal neuronal cells and microglial cells were washed with pre-cooled PBS and fixed with 4% paraformaldehyde. Non-specific antigen binding was blocked using 10% goat serum, followed by incubation with the antibody mixture overnight at 4 °C overnight. Specifically, fixed hippocampal neuronal cells were treated with mouse anti-β3-tubulin antibody (1:100, sc80016, Santa Cruz biotech, USA) in combination with the following antibodies: rabbit anti-p-ErbB4 (1:200, bs-3220R, Bioss, Beijing, China), and rabbit anti-PSD95 (1:200, GB11277-100, Servicebio, Wuhan, China). Fixed microglial cells were treated with mouse anti-IBA1 antibody (1:100, GB15105-100, Servicebio, Wuhan, China) in combination with rabbit anti-phosphorylated nuclear factor-Kappa B (p-NF-κB) antibody (1:200, GB113882-100, Servicebio, Wuhan, China). After being rinsed 3 times with PBS (5 min each), the cells were incubated with a mixture of Alexafluor 488-conjugated goat anti-mouse IgG (1:200, BA1126, Boster, Wuhan, China) and Alexafluor 594-conjugated goat anti-rabbit IgG (1:200, BA1142, Boster,

Wuhan, China) for 2 h. Samples were subsequently mounted using an anti-fade mounting solution containing DAPI (P0131, Beyotime, Shanghai, China). Images were finally acquired using a fluorescence microscope (Axio Imager Z2, Carl Zeiss AG, DE).

### Statistical analysis

Data are expressed as the mean  $\pm$  SEM. Differences among experimental groups were assessed using one-way analysis of variance (ANOVA) followed by Tukey's post hoc test for multiple comparisons. All statistical analyses were performed using GraphPad Prism software (version 8.0). Statistical significance was assigned to a P-value below 0.05.

## Results

### ErbB4 small molecule agonist ameliorates cognitive and behavioral impairments in mice exposed to PS-MPs

Prior to initiating the behavioral experiments, a statistical analysis was conducted to evaluate the weight changes in mice during the administration period. The experimental findings indicated that neither the oral administration of PS-MPs nor the intraperitoneal administration of E4A resulted in significant alterations in the body weight of mice across all groups, suggesting that PS-MPs and E4A did not exert a noticeable impact on the body weight of the mice (Fig. S1A). Behavioral assessments were conducted to examine the potential effects of the ErbB4 small molecule agonist on cognitive and behavioral alterations in mice exposed to PS-MPs. Initially, anxiety levels in the mice were assessed using the open field test. The results demonstrated significantly reduction in the duration of activity in the central area, the distance traveled in the central area, the overall distance covered by the mice, as well as the average movement speed following exposure to PS-MPs when compared to the control group. In contrast, administration of the ErbB4 small molecule agonist significantly increased the duration of activity in the central area, the distance traveled in the central area, the overall distance and the movement speed, compared to the PS-MPs group (Fig. 1A and B, S1B). The findings indicate that administration of an ErbB4 small molecule agonist ameliorates anxiety levels in mice exposed to PS-MPs.

The Y-maze assay was subsequently employed to evaluate the cognitive function of mice, with a specific focus on their learning and memory abilities. The findings revealed that the group exposed to PS-MPs exhibited a significantly lower spontaneous alternation rate compared to the control group. However, treatment with the ErbB4 small molecule agonist resulted in a marked improvement in the spontaneous alternation rate among the PS-MPs exposed mice within the Y-maze paradigm,

indicating an enhancement in their learning and memory functions (Fig. 1C and D).

Following this, an NOR test was conducted to assess the exploratory behavior of the mice. The results demonstrated that, in comparison to the control group, the PS-MPs group showed reduced recognition efficiency for both novel and familiar objects. In contrast, the administration of the ErbB4 small molecule agonist improved the recognition efficiency for these objects (Fig. 1E and F). These findings suggest that the ErbB4 small molecule agonist enhances exploratory behavior in mice exposed to PS-MPs.

In addition, a water maze experiment was conducted to further assess spatial learning and memory performance. The results indicated that the PS-MPs group showed a significant decrease in both the frequency of platform entries and the duration spent on the platform compared to the control group. There was also a reduction in the time and distance of activity within the target quadrant, the effective area, and the platform. However, treatment with the ErbB4 small molecule agonist significantly improved both the frequency of platform entries and the duration spent on the platform in mice exposed to PS-MPs. Moreover, there was an increase in the time and distance of activity within the target quadrant, the effective area, and the platform (Fig. 1G and H). Additionally, the swimming speed was enhanced in mice exposed to PS-MPs and subsequently treated with the ErbB4 receptor agonist (Fig. S1C). These findings imply that activation of ErbB4 via a small molecule agonist augments exploratory behavior, spatial learning and memory capabilities in mice exposed to PS-MPs, thereby improving overall cognitive function.

### ErbB4 small molecule agonist reduces synaptic dysfunction in hippocampal neurons of mice exposed to PS-MPs

To evaluate changes in hippocampal synaptic density, we conducted an examination of the dendritic spines in hippocampal neurons of mice subjected to PS-MPs exposure. Golgi staining analysis indicated that, in comparison to the control group, neurons in the hippocampal regions CA1, CA3, and DG of the PS-MPs group exhibited a reduced dendritic spine density, characterized by a decrease in mature mushroom-shaped spines. In contrast, administration of the ErbB4 small molecule agonist resulted in an increased dendritic spine density and a higher prevalence of mature mushroom-shaped spines in these mice, as illustrated in Fig. 2A and C.

Further investigation using electron microscopy revealed that, relative to the control group, the PS-MPs group displayed a significant reduction in synaptic quantity, an increase in the width of hippocampal synaptic clefts, a decrease in postsynaptic density thickness, and

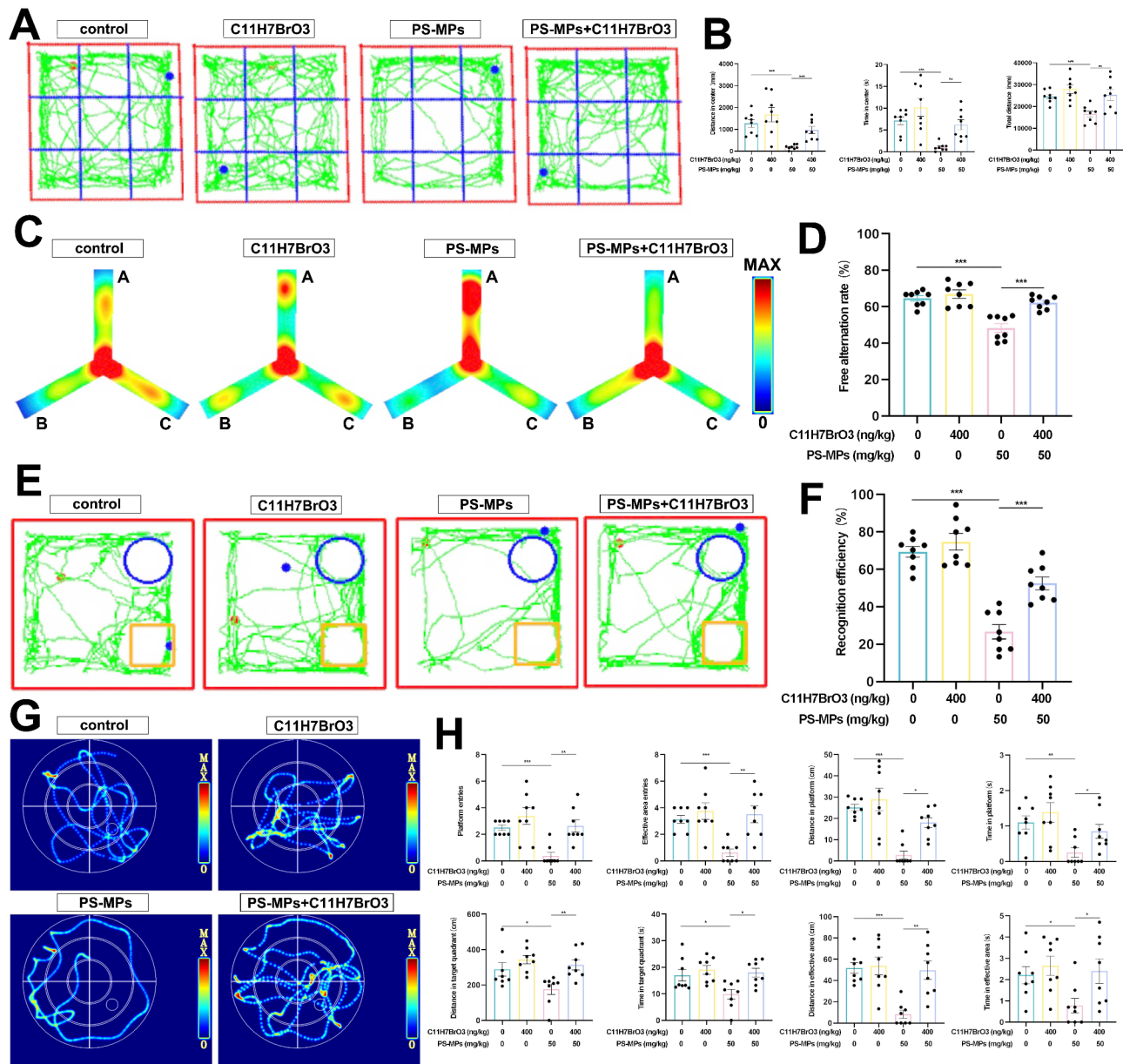


**Fig. 1** ErbB4 small molecule agonist ameliorates cognitive behavioral impairments in mice exposed to PS-MPs. **(A)** Representative traces in open field experiment. **(B)** The statistical analysis related to open field test. **(C)** Representative heat map in Y maze exploration experiment, with arm A denoting the initial arm. **(D)** The rate of spontaneous alternation in Y maze experiment. **(E)** Representative traces from the new object recognition (NOR) experiment. **(F)** Statistical analysis related to the NOR experiment. **(G)** Representative swimming traces from the Morris water maze (MWM) exploration experiment. **(H)** The statistical analysis of MWM exploration test. Statistical analysis was conducted using one-way analysis of variance (ANOVA) followed by Tukey's post hoc test for multiple comparisons, and the data are presented as means  $\pm$  standard error of the mean (SEM). Statistical significance is indicated by \* $p < 0.05$ , \*\* $p < 0.01$ , and \*\*\* $p < 0.001$ , with  $n = 8$  per group

a shortened active zone length at synapses. Conversely, treatment with the ErbB4 small molecule agonist led to an increased number of synapses and an improved synaptic interface structure in mice exposed to PS-MPs (Fig. 3A and B). These findings suggest that the ErbB4 small molecule agonist may play a crucial role in ameliorating synaptic deficits associated with PS-MPs exposure.

Subsequent double-labeled immunofluorescence experiments revealed a reduction in SYP expression in the cortex and hippocampal regions, specifically CA1, CA3, and DG, of mice exposed to PS-MPs compared to the control group. Notably, administration of the ErbB4 small molecule agonist enhanced SYP expression in these PS-MPs-exposed mice. Additionally,  $\beta$ 3-tubulin staining indicated neuronal disruption within the cortical

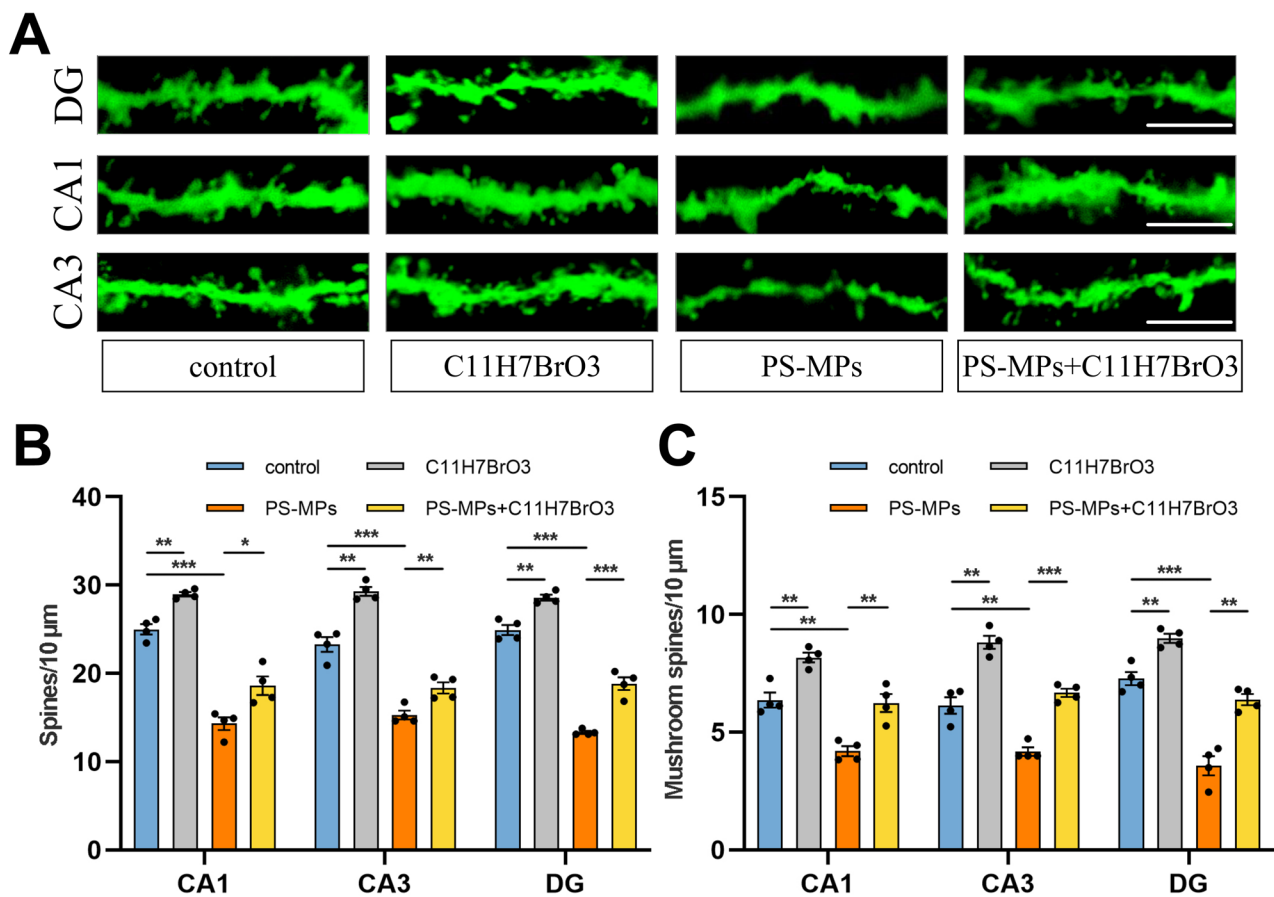


**Fig. 2** ErbB4 small molecule agonist can improve the dendritic spine injury of hippocampal neurons in mice exposed to PS-MPs. **(A)** Representative images of neuronal dendritic segments. scale bar, 10 μm. **(B)** Total dendritic spine density of hippocampal neurons. **(C)** The density of mushroom spines in hippocampal neurons. Statistical analysis was conducted using one-way ANOVA followed by Tukey's post hoc test for multiple comparisons. The results were presented as means ± SEM. Statistical significance is indicated by \* $p < 0.05$ , \*\* $p < 0.01$ , and \*\*\* $p < 0.001$ , with  $n = 4$  per group

and hippocampal regions, resulting in neuronal network interruption in the PS-MPs-exposed mice. This disruption was ameliorated by treatment with the ErbB4 small molecule agonist (Fig. 3C).

To further assess alterations in synaptic protein expression, western blot analysis was performed. The findings indicated a decrease in hippocampal synaptic proteins, including SYP, dedicator of cytokinesis 3 (DOCK3), synaptotagmin 1 (SYT1), and PSD95, growth-associated protein 43 (GAP43), in mice exposed to PS-MPs relative to the control group. Moreover, treatment with the ErbB4 small molecule agonist significantly increased the expression of these synaptic proteins in the hippocampus of PS-MPs-exposed mice (Fig. 3D and E).

Phosphorylation of the transcription factor cyclic AMP-responsive element-binding protein (CREB) is known to enhance synaptic plasticity. Our experimental findings indicated a reduction in hippocampal CREB phosphorylation levels in mice exposed to PS-MPs compared to the control group. However, treatment with ErbB4 small molecule agonist increased the level of

CREB phosphorylation, accompanied with enhanced synaptic plasticity in the hippocampus of mice exposed to PS-MPs (Fig. 3D and E).

The above experimental results suggest that the ErbB4 small molecule agonist can potentially restore synaptic protein expression, and improve synaptic plasticity. Furthermore, it appears to mitigate synaptic dysfunction within the hippocampus of mice exposed to PS-MPs, thereby enhancing the efficiency of synaptic information transmission.

#### ErbB4 small molecule agonist reduces mitochondrial dysfunction in hippocampal neurons of mice exposed to PS-MPs

Electron microscopy analysis revealed that hippocampal neurons in mice exposed to PS-MPs displayed marked degenerative features, such as nuclear membrane rupture, cell membrane rupture, reduced mitochondrial count, significant swelling, cristae disruption, severe mitochondrial vacuolization, and structural disarray, in comparison to the control group (Fig. 4A and B).



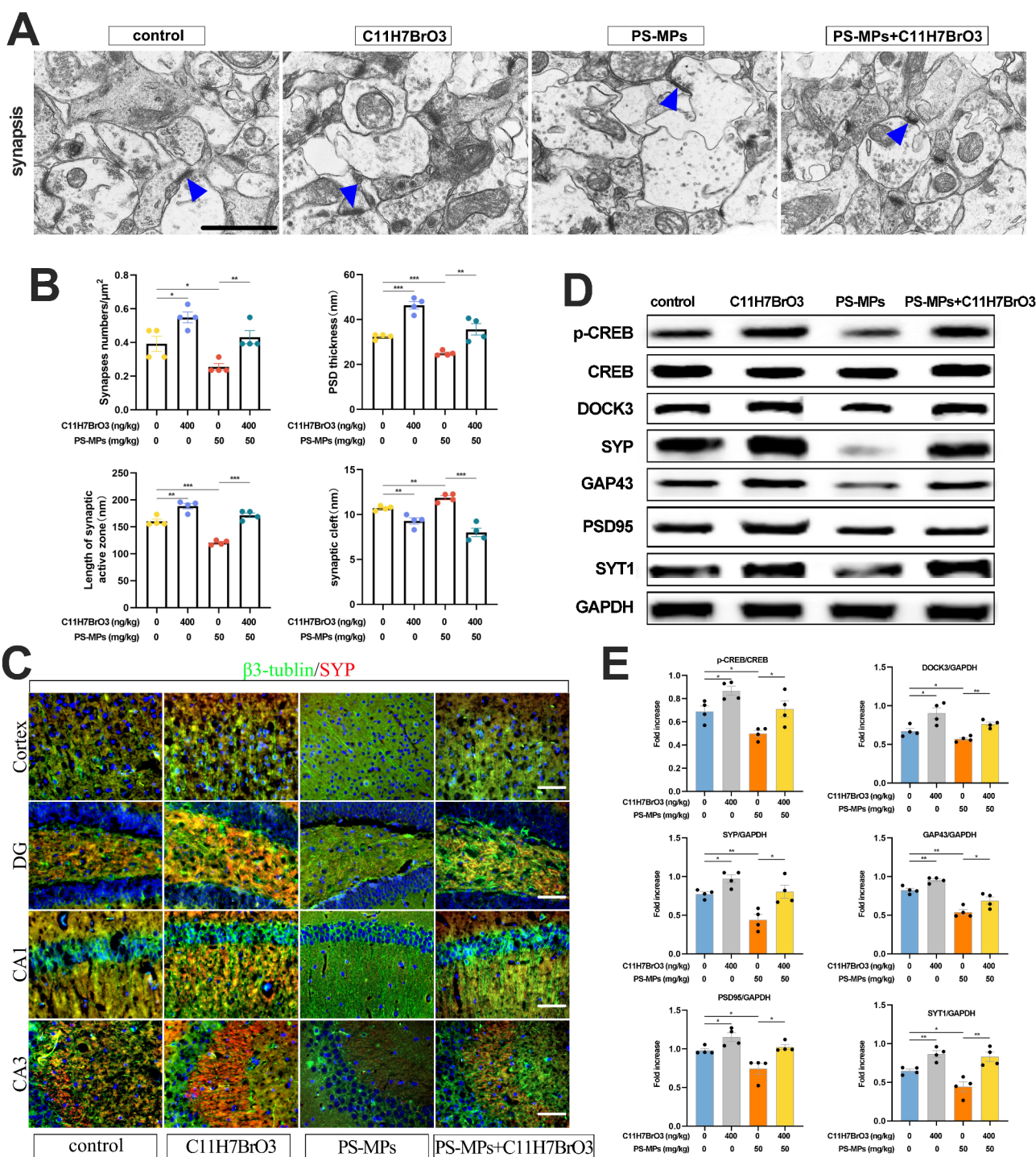


**Fig. 3** ErbB4 small molecule agonist can improve synaptic dysfunction of hippocampal neurons in mice exposed to PS-MPs. **(A)** The ultrastructural analysis of hippocampal neuron synapses was performed using transmission electron microscopy (TEM). **(B)** Statistical analyses were conducted on the synaptic data of hippocampal neurons. **(C)** Immunofluorescence was employed to detect the levels of synaptophysin (SYP) and  $\beta 3$ -tubulin. **(D)** Western blot analysis was utilized to assess the protein levels of synapse-associated proteins, including DOCK3, p-CREB, CREB, SYP, GAP43, PSD95, and SYT1 in hippocampal neurons. **(E)** Statistical analyses of these protein levels were performed using one-way ANOVA with Tukey's multiple comparison test. The synaptic structure was examined at a magnification of 10,000 $\times$ , with a scale bar of 1  $\mu\text{m}$ . Results are expressed as means  $\pm$  SEM. Immunofluorescence labeling was as follows: SYP in red and  $\beta 3$ -tubulin in green, with a scale bar of 20  $\mu\text{m}$ . Statistical significance was indicated by \* $p < 0.05$ , \*\* $p < 0.01$ , and \*\*\* $p < 0.001$ , with a sample size of  $n = 4$  per group



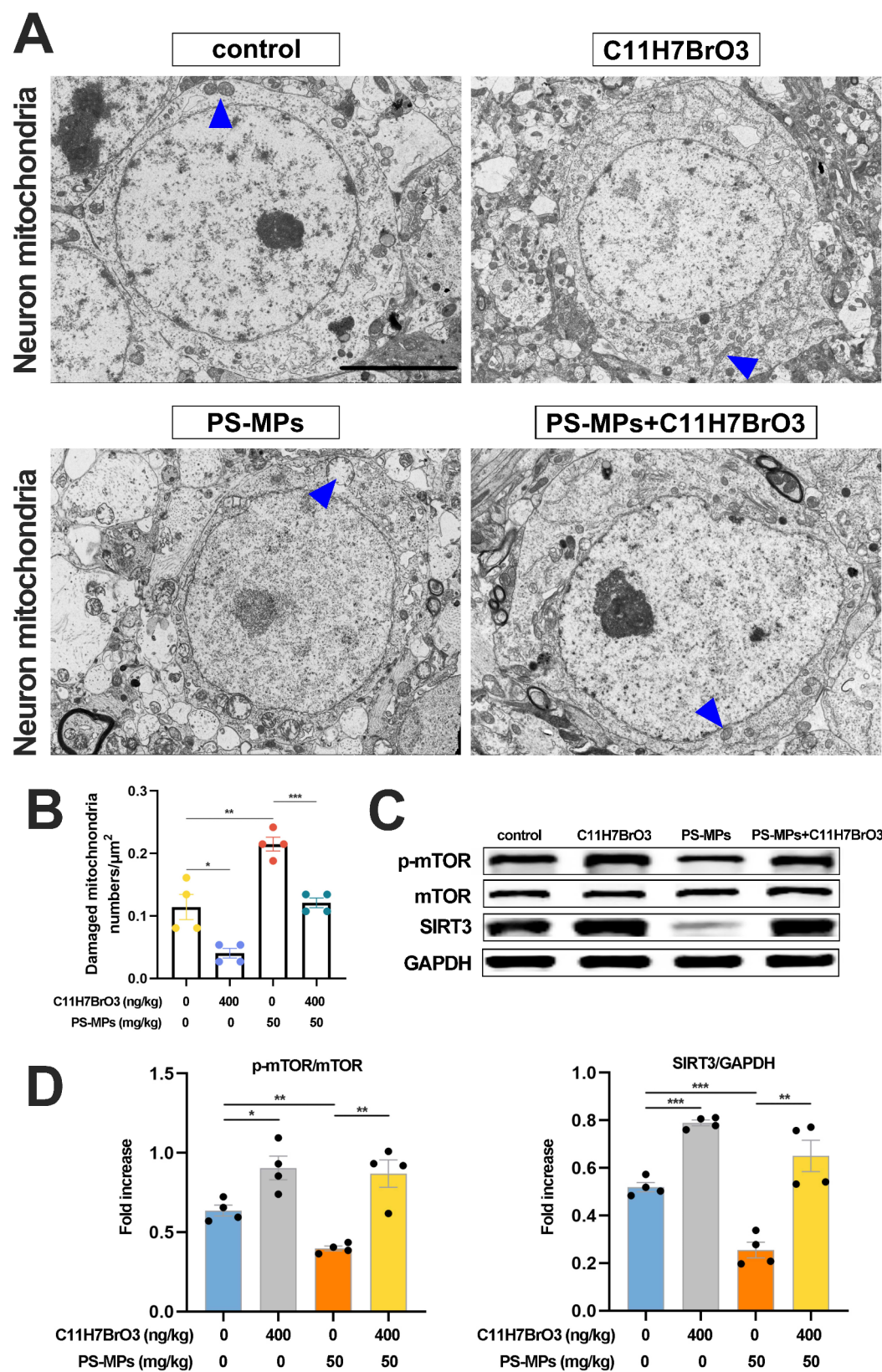


**Fig. 4** (See legend on next page.)

(See figure on previous page.)

**Fig. 4** ErbB4 small molecule agonist can improve mitochondrial damage in hippocampal neurons of mice exposed to PS-MPs. **(A)** The ultrastructural integrity of hippocampal neuronal mitochondria was evaluated using transmission electron microscopy (TEM). **(B)** Statistical analyses were performed on data pertaining to the hippocampal neuronal mitochondria. **(C)** The expression levels of mitochondria-associated proteins, including phosphorylated mTOR (p-mTOR), mTOR, and SIRT3, in the hippocampus of mice were quantified via western blot analysis. **(D)** Statistical analyses of these protein expression levels were conducted using one-way ANOVA followed by Tukey's post hoc test for multiple comparisons. The original magnification for mitochondrial imaging was 2000 $\times$ , with a scale bar of 5  $\mu$ m. Data are presented as means  $\pm$  SEM. Statistical significance was indicated by \* $p < 0.05$ , \*\* $p < 0.01$ , and \*\*\* $p < 0.001$ , with a sample size of  $n = 4$  per group

However, following treatment with the ErbB4 small molecule agonist, the hippocampal neurons of mice exposed to PS-MPs exhibited normal morphology, an abundance of mitochondria, and intact nuclear membranes. Subsequent analysis of the number of damaged mitochondria per unit area demonstrated a significant increase in mitochondrial damage in mice exposed to PS-MPs compared to the control group. However, this phenomenon was reversed upon administration of the ErbB4 small molecule agonist (Fig. 4A and B).

Sirtuin 3 (SIRT3) is a mitochondrial protein integral to various aspects of mitochondrial biology, and its dysregulation can result in mitochondrial dysfunction. Similarly, the mammalian target of rapamycin (mTOR) phosphorylation level plays a crucial role in the regulation of mitochondrial function. In this study, the expression levels of SIRT3 and p-mTOR proteins were found to be reduced in mice exposed to PS-MPs compared to the control group. Notably, administration of the ErbB4 small molecule agonist led to an increase in the expression of SIRT3 and p-mTOR proteins in PS-MPs-exposed mice (Fig. 4C and D). These findings indicate that the ErbB4 small molecule agonist may mitigate hippocampal mitochondrial damage and enhance mitochondrial stability.

#### **ErbB4 small molecule agonist enhances ErbB4 signaling pathway in the hippocampus of mice exposed to PS-MPs**

Given ErbB4's role in synaptic plasticity regulation, we investigated changes in the ErbB4 pathway using immunofluorescence and western blot analyses. Double-labelling immunofluorescence experiments revealed a reduction in the co-expression of phosphorylated ErbB4 (p-ErbB4) and  $\beta$ 3-tubulin proteins in the cortical, hippocampal CA1, CA3, and DG regions of PS-MP-exposed mice compared to the control group. However, treatment with ErbB4 small molecule agonist resulted in an increase in co-expression (Fig. 5A).

Subsequently, we observed a reduction in the phosphorylated expression of ErbB4, accompanied by decreased phosphorylation levels of downstream signaling molecules such as signal transducer and activator of transcription 5 (STAT5), protein kinase B (Akt), extracellular regulated protein kinases (Erk), and cellular Src (c-Src) in mice exposed to PS-MPs compared to the control group. Notably, this effect was reversed following administration of the ErbB4 small molecule agonist (Fig. 5B and C). These findings indicate that the ErbB4

small molecule agonist can enhance the expression of the ErbB4 signaling pathway in the hippocampus of mice exposed to PS-MPs.

#### **ErbB4 small molecule agonist reduces the activation of the TLR4-NF- $\kappa$ B-NLRP3 pathway in the hippocampus of mice exposed to PS-MPs, thereby decreasing neuroinflammation**

Our additional investigations revealed an increase in (IBA1)-positive microglial cells with enlarged cytoplasm and shortened processes, which were clustered in the hippocampal CA1, CA3, DG, and cortical regions of mice exposed to PS-MPs compared to the control group. Compared to the PS-MPs group, mice administered with the ErbB4 small molecule agonist exhibited a reduction in activated microglial cells within these brain regions. The alterations observed in astrocytes were consistent with those noted in microglial cells (Fig. 6A and B). Furthermore, western blot analysis revealed increased expression levels of GFAP and IBA1 proteins in the hippocampus of mice exposed to PS-MPs relative to the control group, corroborating the immunofluorescence findings. Treatment with the ErbB4 small molecule agonist resulted in a reduction in GFAP and IBA1 protein expression levels (Fig. 6C and D).

A more comprehensive analysis of inflammatory pathway factors demonstrated that the protein expression levels of hippocampal Toll-like receptor 4 (TLR4) and p-NF- $\kappa$ B subunit were elevated in the PS-MPs group compared to the control group. Additionally, the protein expression levels of downstream NLR family pyrin domain containing 3 (NLRP3) inflammasome components, including NLRP3, apoptosis-associated speck-like protein containing a CARD (ASC), and cleaved cysteinyl aspartate specific proteinase 1 (cl-Caspase-1), as well as the expression of catalytically produced pro-inflammatory cytokine interleukin-1 beta (IL-1 $\beta$ ), were also increased in the PS-MPs group. In contrast, treatment with the ErbB4 small molecule agonist led to a reduction in the activation level of the TLR4-NF- $\kappa$ B-NLRP3 signaling pathway in the hippocampus of mice exposed to PS-MPs (Fig. 6C and D). The findings indicate that administering an ErbB4 small molecule agonist may mitigate the activation of the TLR4-NF- $\kappa$ B-NLRP3 signaling pathway, thereby reducing neuroinflammation in mice exposed to PS-MPs.



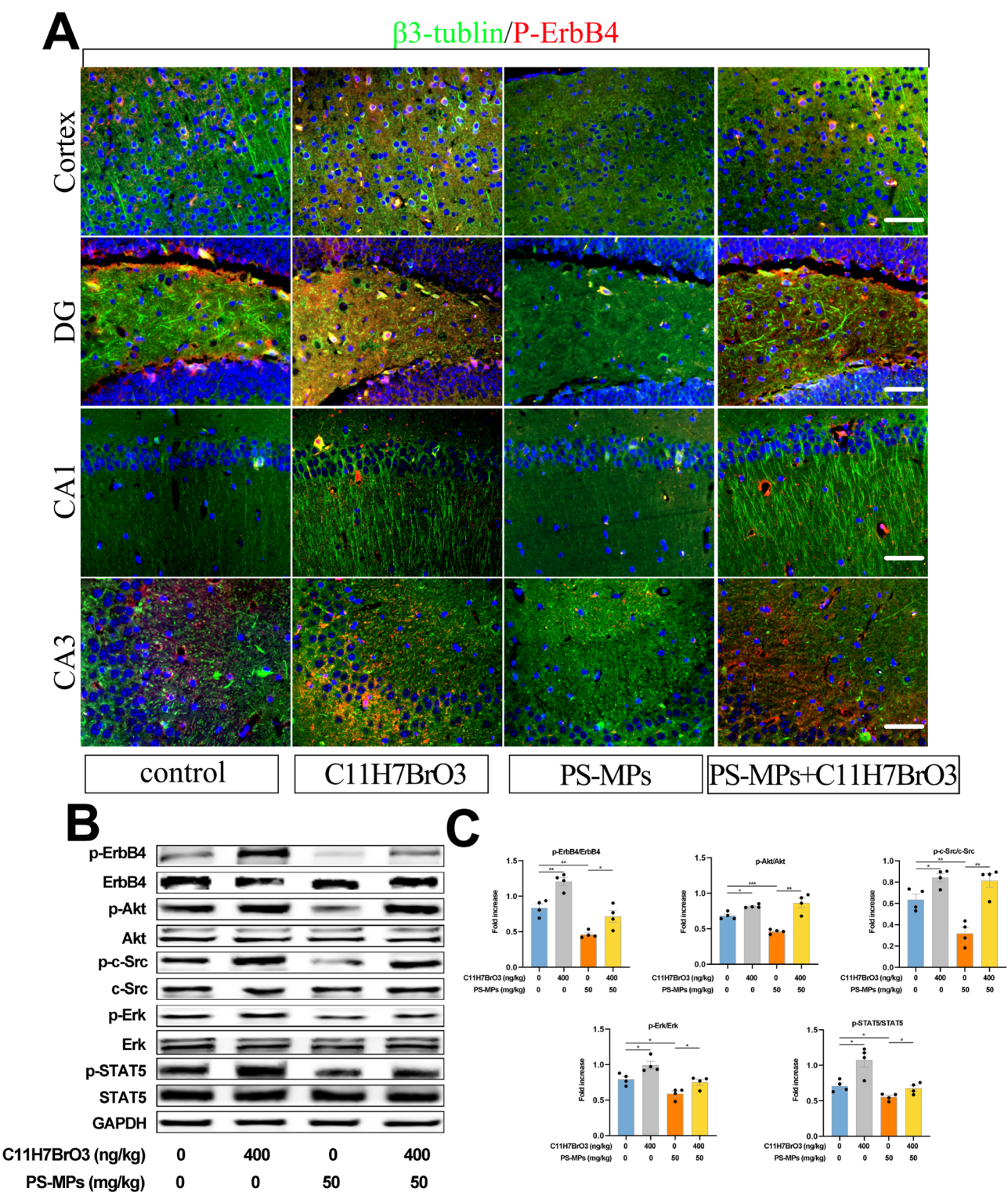


**Fig. 5** ErbB4 small molecule agonist enhances the ErbB4 signaling pathway in hippocampus of mice exposed to PS-MPs. **(A)** Immunofluorescence was used to detect levels of phosphorylated ErbB4 (p-ErbB4) and  $\beta$ 3-tubulin. **(B)** Protein levels associated with the ErbB4 signaling pathway in the hippocampus of mice were assessed through western blot analysis. **(C)** A statistical analysis was performed on the data derived from protein levels, employing one-way ANOVA with Tukey's multiple comparison tests. The p-ErbB4 is represented in red, while  $\beta$ 3-tubulin is depicted in green, with a scale bar of 20  $\mu$ m. The results are expressed as means  $\pm$  SEM, with significance levels indicated by \* $p < 0.05$ , \*\* $p < 0.01$ , and \*\*\* $p < 0.001$ . Each experimental group comprised  $n = 4$  samples

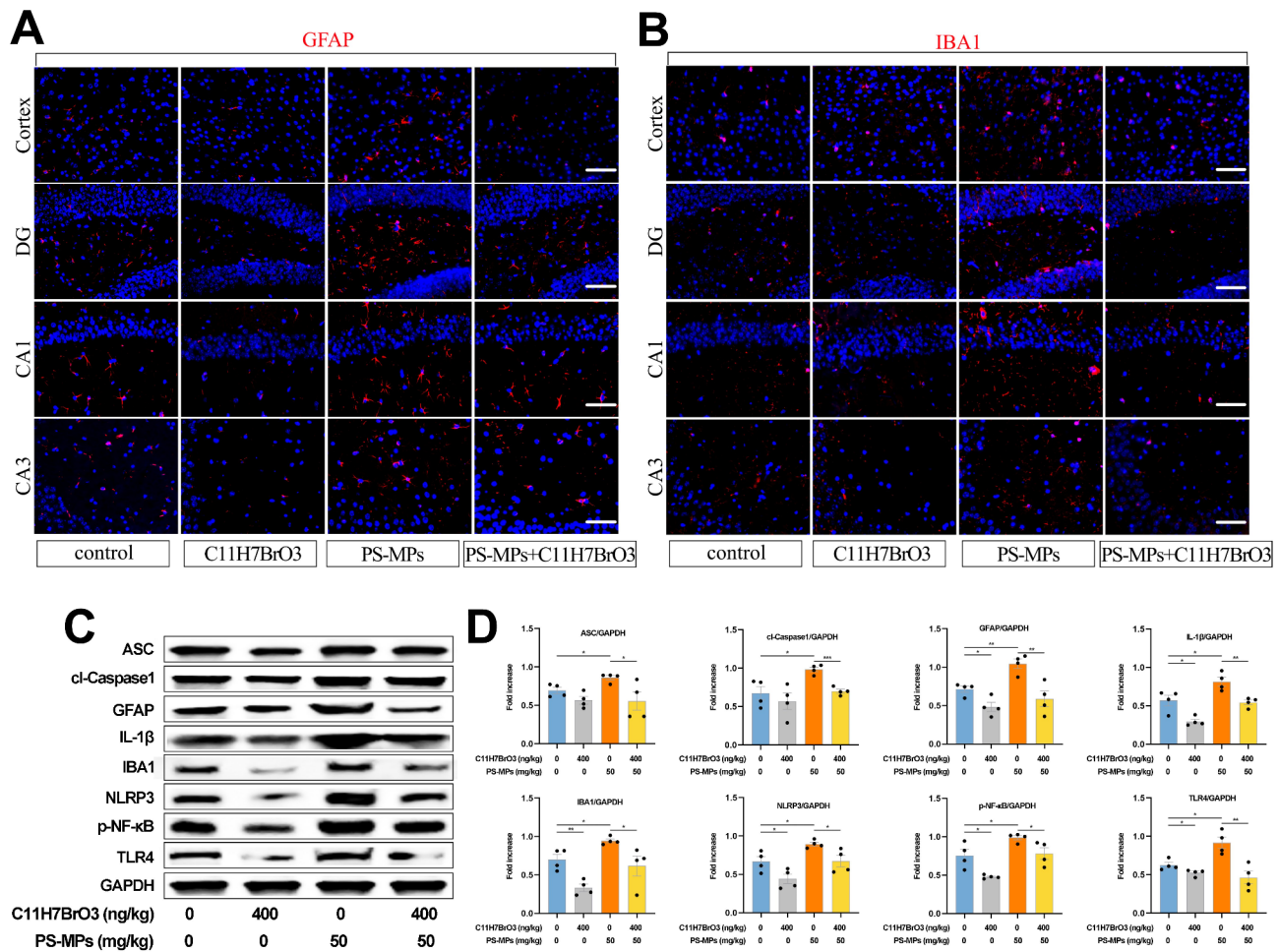


**Fig. 6** ErbB4 small molecule agonist can improve hippocampal neuroinflammation in mice exposed to PS-MPs via the TLR4/NLRP3 pathway. **(A)** Levels of IBA1 were detected through immunofluorescence staining. **(B)** Levels of GFAP were detected through immunofluorescence staining. **(C)** Western blot analysis was utilized to detect protein levels associated with the TLR4/NLRP3 signaling pathway in the hippocampus of mice. **(D)** Statistical chart was generated to display the protein levels of TLR4/NLRP3. GFAP and IBA1 are both indicated in red, with a scale bar of 20  $\mu$ m. Statistical analysis was conducted using one-way ANOVA followed by Tukey's post hoc test for multiple comparisons, and the data are reported as means  $\pm$  SEM, with significance levels denoted as \* $p$  < 0.05, \*\* $p$  < 0.01, and \*\*\* $p$  < 0.001. Each group comprised  $n$  = 4 samples

### ErbB4 small molecule agonist can alleviate hippocampal neuron damage under PS-MPs pathological conditions through the ErbB4 signaling pathway

To examine the impact of our ErbB4 small molecule agonist on mice exposed to PS-MPs, we developed an in vitro model simulating ErbB4 small molecule agonist treatment under PS-MPs pathological conditions. The findings indicated that, relative to the control group, the PS-MPs group exhibited reduced phosphorylation levels of ErbB4 and associated pathway molecules, including Akt, c-Src, Erk. Conversely, when compared to the PS-MPs group, the PS-MPs + C11H7BrO3 group demonstrated increased phosphorylation levels of ErbB4 and its pathway-related molecules (Fig. 7A and B). The results were corroborated by immunofluorescence co-staining experiments (Fig. S2A), indicating that the ErbB4 small molecule agonist can activate the ErbB4 signaling

pathway in hippocampal neurons under pathological conditions induced by PS-MPs. Relative to the control group, the PS-MPs group exhibited a slight reduction in the SIRT3 protein level (Fig. 7C and D). Furthermore, levels of synaptic-related proteins, including DOCK3, SYP, GAP43, and PSD95, were diminished, while the level of the apoptosis protein cl-Caspase3 increased (Fig. 7A and D). These observations were further substantiated by immunofluorescence co-staining experiments (Fig. S2B), suggesting a correlation between apoptosis, synaptic dysfunction, and mitochondrial impairment induced by PS-MPs damage. Upon treatment with the agonist under PS-MPs pathological conditions, the PS-MPs + C11H7BrO3 group exhibited increased expression levels of mitochondrial and synaptic-related proteins and decreased levels of apoptosis proteins compared to the PS-MPs group (Fig. 7A and D).



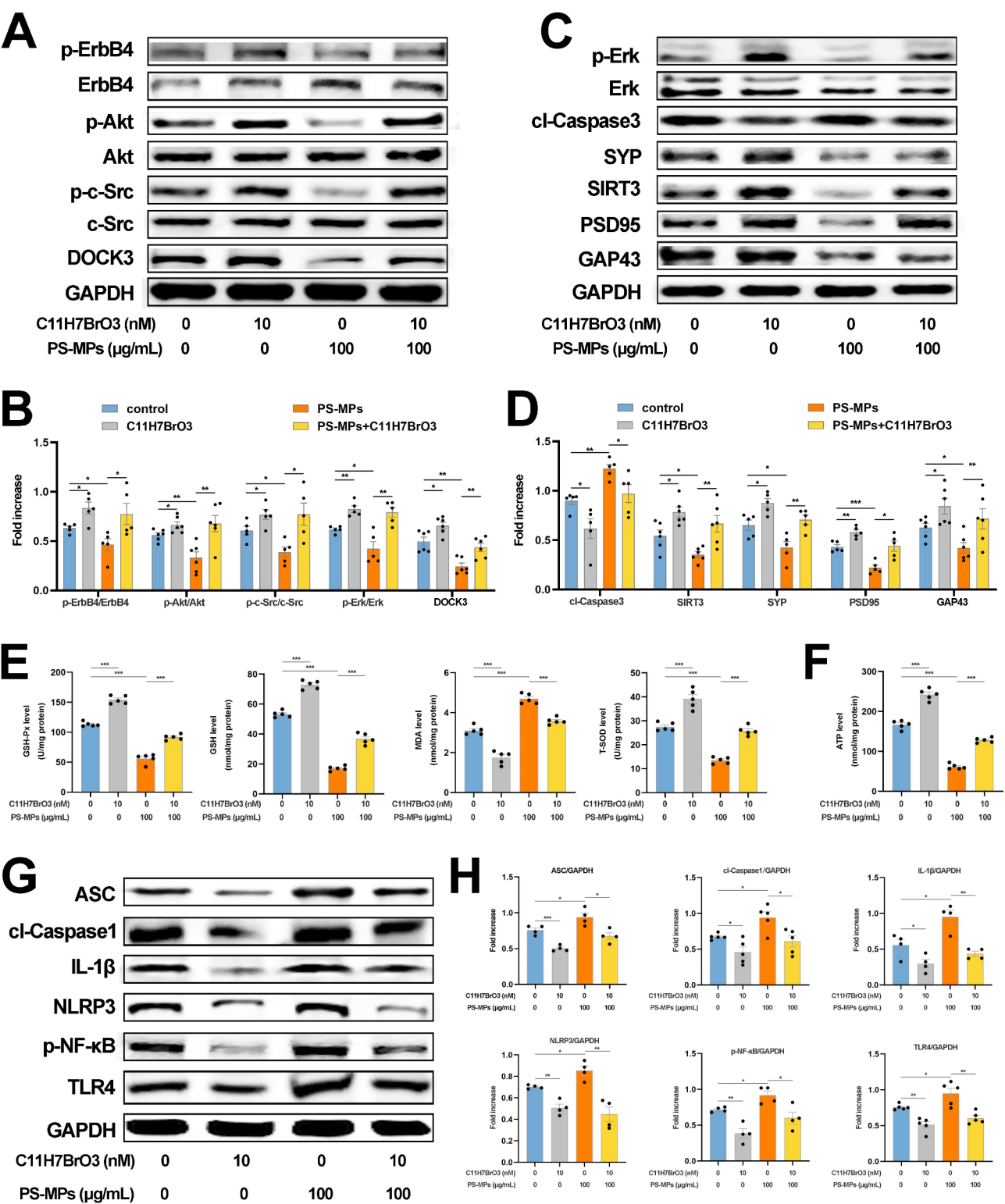


**Fig. 7** (See legend on next page.)

Mitochondrial redox imbalance is an important mechanism for oxidative stress-induced cell damage. In this study, we further examined the level of oxidative stress in hippocampal neurons. We found that compared to the control group, the PS-MPs group showed a decrease in oxidative stress-related T-SOD, GSH and GSH-Px, an increase in MDA levels, alongside diminished ATP levels (Fig. 7E and F). In comparison to the PS-MPs group, the



(See figure on previous page.)

**Fig. 7** The ErbB4 small molecule agonist ameliorates hippocampal neuron damage under pathological conditions induced by PS-MPs in vitro via the ErbB4 signaling pathway, and concurrently attenuates microglial activation through the TLR4/NLRP3 signaling pathway. **(A–D)** Following exposure to PS-MPs at a concentration of 100 µg/mL for 24 h, hippocampal neurons were subsequently treated with C11H7BrO3 at a concentration of 10 nM for an additional 24 h. **(A, C)** Protein expression levels associated with the ErbB4 signaling pathway, mitochondrial function, apoptosis, and synaptic integrity in hippocampal neurons were quantified using Western blot analysis. **(B, D)** Statistical representations of these protein expression levels were depicted in graphical form. **(E)** Oxidative stress markers in hippocampal neurons, including total superoxide dismutase (T-SOD), glutathione (GSH), glutathione peroxidase (GSH-Px), and malondialdehyde (MDA) levels, were evaluated. **(F)** Intracellular ATP levels in hippocampal neurons were also measured. **(G–H)** Microglial cells were co-cultured with supernatants derived from treated hippocampal neurons for 24 h. **(G)** Protein expression levels related to the TLR4/NLRP3 signaling pathway in microglial cells were assessed via Western blot analysis. **(H)** Statistical representations of these protein expression levels were also depicted in graphical form. Statistical analysis was conducted using one-way ANOVA followed by Tukey's post hoc test for multiple comparisons, and data are presented as means ± SEM. Significance levels were denoted as \* $p < 0.05$ , \*\* $p < 0.01$ , \*\*\* $p < 0.001$ . A minimum sample size of  $n = 4–6$  per group was utilized

PS-MPs + C11H7BrO3 group exhibited elevated levels of T-SOD, GSH, and GSH-Px, alongside reduced MDA levels and increased ATP concentrations (Fig. 7E and F). These findings indicate that the ErbB4 small molecule agonist may mitigate apoptosis, facilitate the restoration of mitochondrial and synaptic functions, and sustain redox homeostasis, in addition to enhancing ATP energy supply in hippocampal neurons under pathological conditions induced by PS-MPs.

#### Under PS-MPs pathological conditions, ErbB4 small molecule agonist can alleviate the impact of hippocampal neurons on microglial inflammation

It remains unclear whether our ErbB4 small molecule agonist can mitigate microglial inflammation, despite their known efficacy in alleviating hippocampal neuron damage under pathological conditions induced by PS-MPs. In order to investigate this issue, we collected supernatants from hippocampal neurons treated with PS-MPs, both in the presence and absence of the ErbB4 small molecule agonist, to evaluate their impact on microglial activation. Initially, immunofluorescence analysis revealed that exposure to PS-MPs resulted in enlarged microglial cell bodies, elongated protrusions, and the nuclear-cytoplasmic translocation of p-NF-κB. However, treatment with the ErbB4 small molecule agonist restored microglial morphology to normal and inhibited nuclear translocation (Fig. S3).

To further elucidate these observations, we conducted molecular biology experiments. Our results indicate that, compared to the control group, the PS-MPs group exhibited increased expression levels of TLR4 and p-NF-κB proteins in microglial cells. Additionally, the protein expression of downstream inflammatory components NLRP3, ASC, and cl-Caspase-1 was also elevated (Fig. 7G and H). Furthermore, the expression level of IL-1β was observed to be increased (Fig. 7G and H). In contrast, the PS-MPs + C11H7BrO3 group exhibited reduced protein expression levels of TLR4 and p-NF-κB in microglia, along with diminished expression of downstream NLRP3 inflammasome components, including NLRP3, ASC, and cl-Caspase-1 (Fig. 7G and H). Additionally, the

expression level of IL-1β was also decreased (Fig. 7G and H). These findings suggest that the ErbB4 small molecule agonist mitigates the effects of damaged hippocampal neurons on microglial inflammation within the pathological context of PS-MPs. Consequently, it can be inferred that the ErbB4 small molecule agonist not only attenuates hippocampal neuron damage under PS-MPs pathological conditions but also reduces microglial inflammation.

In summary, the schematic diagram elucidates the therapeutic effects of targeted ErbB4 receptor activation on hippocampal neuronal damage, neuroinflammation, and cognitive functions in mice exposed to PS-MPs (Fig. 8).

#### Discussion

Research indicates that neuronal damage significantly contributes to cognitive dysfunction resulting from exposure to PS-MPs [45]. The neuronal damage is characterized by mitochondrial dysfunction, diminished synaptic plasticity, and abnormal regulation of glial cells, which collectively can intensify the inflammatory response in microglia [46, 47]. The NRG1/ErbB4 signaling pathway is crucial for neuronal plasticity and cognitive function regulation [48]. This study demonstrates that employing the ErbB4 small molecule agonist may offer a potential therapeutic approach for cognitive dysfunction induced by PS-MPs exposure.

PS-MPs represent a novel class of environmental pollutants capable of entering the human body via the food chain. Notably, microplastics ranging from 1 to 5 µm in diameter are more closely associated with neurotoxicity, with an average diameter of approximately 2 µm found in edible fruits and vegetables [29]. Damage to hippocampal neurons leads to a decline in synaptic plasticity, which is a critical factor in the development of cognitive impairment [49–51]. This study identified a decline in cognitive function in mice following the administration of 2 µm PS-MPs, indicating a potential link between PS-MPs-induced cognitive impairment and neuronal damage in the hippocampus. Golgi staining and electron microscopy analyses revealed that exposure to PS-MPs reduced hippocampal neuron count and disrupted neuronal ultrastructure, evidenced by lower synaptic density

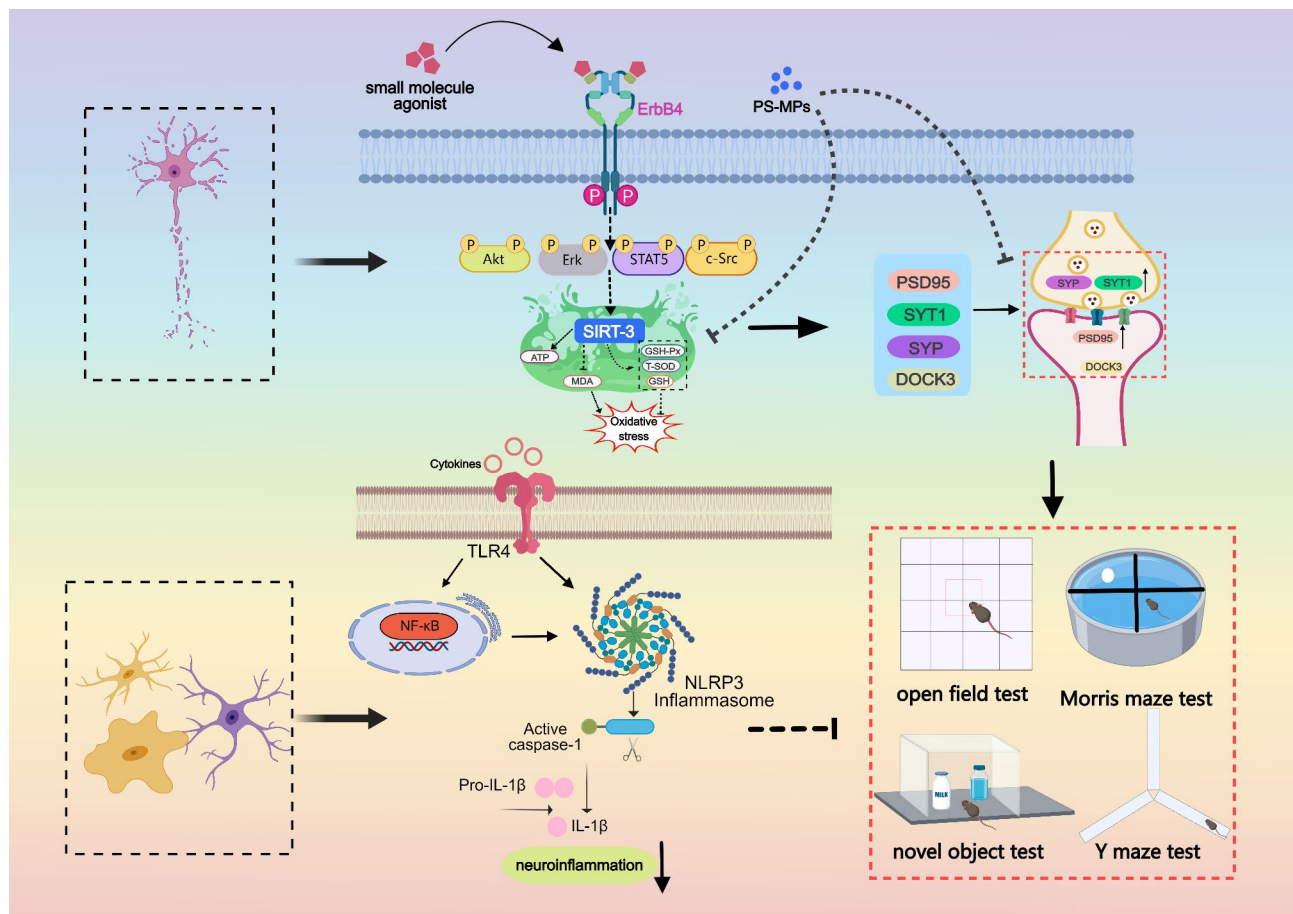


**Fig. 8** The schematic diagram illustrates the impact of targeted activation of ErbB4 receptor on hippocampal neuronal damage, neuroinflammation, and cognitive functions in mice exposed to PS-MPs. The small molecule ErbB4 receptor agonist (E4A) binds to the ErbB4 receptor, initiating its downstream signaling pathway. This activation leads to the upregulation of SIRT3 protein expression, which enhances mitochondrial redox homeostasis, increases ATP production, and ameliorates mitochondrial dysfunction. Additionally, there is an upregulation of synaptic-related proteins, which contributes to the repair of synaptic damage and enhancement of synaptic function. As hippocampal neuronal function improves, the activation of the TLR4 receptor by pro-inflammatory factors in microglia is reduced, resulting in diminished phosphorylation of NF-κB and decreased activation of the NLRP3 inflammasome towards Caspase-1. Consequently, there is a reduction in the conversion of the IL-1β precursor to its mature form, thereby alleviating hippocampal neuroinflammation and ultimately enhancing the learning and cognitive functions of PS-MPs-exposed mice. The diagram was created with MedPeer ([www.medpeer.cn](http://www.medpeer.cn))

and connections. Further examination demonstrated a reduction in the density of dendritic spines, particularly mushroom spines, subsequent to PS-MPs exposure. Concurrently, PS-MPs exposure led to a decrease in the expression of SYP, DOCK3, SYT1 and PSD95 culminating in synaptic damage.

NRG1-ErbB4 signaling is critically involved in various physiological functions of the nervous system, encompassing neuronal differentiation and migration, synaptic plasticity, and the synthesis and secretion of neurotransmitters [52]. Specifically, hippocampal NRG1-ErbB4 signal transduction plays a pivotal role in modulating cognitive processes by regulating neural networks and the synchronous activities of pyramidal cells [53]. Disruptions in NRG1-ErbB4 signaling can result in hippocampal-dependent memory impairments [17]. In the

present study, we initially observed that exposure to PS-MPs resulted in diminished activation of ErbB4 receptor within the hippocampus of mice. Concurrently, there was a reduction in the phosphorylation levels of downstream signaling molecules such as Erk, Akt, STAT5, and c-Src. However, administration of ErbB4 small molecule agonist led to an increase in the phosphorylation levels of ErbB4-related pathway proteins. These findings suggest that this agonist can activate ErbB4 and its downstream pathways, thereby ameliorating the cognitive deficits induced by PS-MPs exposure. This is achieved by enhancing neuronal numbers and improving the ultrastructure of neurons and synapses.

Mitochondrial homeostasis plays a crucial role in sustaining synaptic efficacy [13]. Mitochondria, predominantly synthesized in neuronal cell bodies, are essential

for providing energy required for various synaptic functions, including synaptic transmission, growth, and vesicle formation [54]. Following mitochondrial damage, the ATP supply to synapses diminishes, leading to synaptic degeneration. Such damage to synaptic mitochondria disrupts REDOX homeostasis, impairing neurotransmission and exacerbating cognitive dysfunction [55]. An electron microscopy result revealed that exposure to PS-MPs induced ultrastructural damage, mitochondrial vacuolation, and neurodegeneration in the hippocampal neurons of mice, thereby affecting synaptic information transmission. In vitro experiments further demonstrated that PS-MPs exposure led to REDOX imbalance and a reduction in intracellular ATP levels in hippocampal neurons. SIRT3 is implicated in the regulation of mitochondrial dynamics by activating the mTOR signaling pathway, playing a significant role in maintaining mitochondrial stability and quality [56, 57]. In this study, we observed that exposure to PS-MPs resulted in a reduction of SIRT3 levels and a decrease in mTOR phosphorylation, indicating that PS-MPs may contribute to mitochondrial dysfunction in mice via the SIRT3/mTOR signaling pathway. ErbB4 plays a role in the regulation of mitochondrial function, and its deficiency may be associated with a loss of mitochondrial membrane potential [19]. The ErbB4 small molecule agonist was found to counteract the loss of mitochondrial proteins induced by PS-MPs exposure, facilitate improvements in synaptic ultrastructure, and support the maintenance of redox homeostasis. We thus propose that targeted activation of ErbB4 receptor could enhance mitochondrial functional homeostasis by activating the SIRT3/mTOR pathway.

Neuroinflammation is implicated in the onset and progression of cognitive disorders, with the release of pro-inflammatory cytokines contributing to neuronal damage [11]. In this study, PS-MPs exposure was found to promote the over-activation of hippocampal microglia and astrocytes in mice, leading to a significant increase in their numbers. It was observed that exposure to PS-MPs led to increased phosphorylation levels of TLR4 and NF- $\kappa$ B, along with elevated expression levels of ASC, cl-Caspase-1, and NLRP3 in the hippocampus, ultimately causing a cascaded amplification of IL-1 $\beta$ . The NLRP3 inflammasome is integral to the activation of Caspase-1, which is essential for the conversion of IL-1 $\beta$  precursors into their mature form. This process is fundamental to microglia-mediated inflammatory cascade responses and their related cognitive impairments [58, 59]. Research has shown that an escalation in the inflammatory cascade can lead to excessive synapse pruning, resulting in synaptic dysfunction [60]. This understanding is instrumental in investigating the pathogenic mechanisms underlying neuroinflammation. Consequently, we hypothesize that cognitive impairments induced by PS-MPs may be

associated with synaptic dysfunction stemming from the inflammatory cascade. Prior research has identified disruptions in NRG1-ErbB4 signaling within the hippocampal region of mice subjected to systemic inflammation [17], suggesting a potential involvement of ErbB4 in neuroinflammatory processes. The administration of ErbB4 small molecule agonist was found to mitigate the increased TLR4 and NF- $\kappa$ B induced by PS-MPs exposure, reduce the activation of microglia and astrocytes, inhibit the activation of the NLRP3 inflammasome, and consequently decrease the release of pro-inflammatory factors.

ErbB4 receptors are predominantly localized in neurons [61]. Nevertheless, the mechanism by which the ErbB4 small molecule agonist operates under pathological conditions induced by PS-MPs remains insufficiently understood. Our in vitro experiments further revealed that the supernatant from hippocampal neurons exposed to PS-MPs and subsequently treated with an ErbB4 small molecule agonist can mitigate microglial inflammation. This inflammation is otherwise induced by the supernatant from hippocampal neurons exposed solely to PS-MPs. This suggests that the ErbB4 small molecule agonist may ameliorate microglial inflammation by enhancing neuronal function. A reduction in ATP levels within the neuronal supernatant appears to be a significant factor in mitigating microglial inflammation, which will be the focus of our subsequent investigations.

PS-MPs are primarily ingested orally and have been shown to impact nervous system function, particularly memory and cognitive processes [62, 63]. This study demonstrates that the ErbB4 small molecule agonist administration can effectively mitigate synaptic dysfunction induced by PS-MPs exposure in mice, thereby indirectly reducing neuroinflammation and alleviating cognitive impairment. However, the precise mechanisms through which the ErbB4 small molecule agonist ameliorates PS-MPs-induced cognitive dysfunction require further investigation. This research provides a significant foundation for the development of nutritional and pharmacological interventions targeting ErbB4 receptor, thus facilitating addressing the adverse effects of PS-MPs on the nervous system.

### Supplementary Information

The online version contains supplementary material available at <https://doi.org/10.1186/s12974-025-03406-6>.

Supplementary Material 1

Supplementary Material 2

### Author contributions

C.L.: Conceptualization, Experimental design, Experiment progress, Data analysis, Writing - original draft, Writing - review & editing. Y.Z.: Conceptualization, Data analysis, Writing - original draft. W.Z.: Experiment

progress. J-J.D.: Experiment progress. Q.L.: Experiment progress. J.H.: Experiment progress. Z-F.L.: Experiment progress. Y-K.M.: Experiment progress. C-M.Q.: Data analysis. C.C.: Data analysis. S-X.C.: Writing - review & editing. L.Y.: Writing - review & editing. Y-Q.S.: Writing - review & editing. W-J.Z.: Experimental design, Writing - review & editing, Funding acquisition. All authors read and approved the final manuscript.

### Funding

This research was funded by Jiangsu Province Shuangchuang Talent Plan (grant no. JSSCRC 2021533), National Natural Science Foundation of China (grant no. 82301581), the Research Start-up Fund of Jiangnan University (grant no. 1285081903200020), Guizhou Nursing Vocational College Foundation (gzhljy 2023-04), and Science and Technology Foundation of Guizhou Provincial Health Committee (gzwkj 2022 – 518).

### Data availability

No datasets were generated or analysed during the current study.

### Declarations

### Ethical approval

All procedures were conducted according to the Ethics Committee of Jiangnan University Wuxi Medical College.

### Competing interests

The authors declare no competing interests.

### Author details

<sup>1</sup>MOE Medical Basic Research Innovation Center for Gut Microbiota and Chronic Diseases, Department of Cell Biology, Wuxi School of Medicine, Jiangnan University, Wuxi, Jiangsu, China

<sup>2</sup>School of Basic Medical Sciences, Experimental Center for Medical Research, Neurologic Disorders and Regeneration Repair Lab of Shandong Higher Education, Shandong Second Medical University, Weifang, Shandong, China

<sup>3</sup>Department of Pathogen Biology, Guizhou Nursing Vocational College, Guiyang, Guizhou, China

<sup>4</sup>Experimental Center for Medical Research, Shandong Second Medical University, Weifang, Shandong, China

<sup>5</sup>Rehabilitation Therapy, Medical School, Weifang University of Science and Technology, Weifang, Shandong, China

<sup>6</sup>MOE Medical Basic Research Innovation Center for Gut Microbiota and Chronic Diseases, Department of Neurodegeneration and Neuroinjury, Wuxi School of Medicine, Jiangnan University, Wuxi, Jiangsu, China

<sup>7</sup>The First Affiliated Hospital, Department of Neurology, Multi-Omics Research Center for Brain Disorders, Hengyang Medical School, University of South China, Hengyang, Hunan, China

<sup>8</sup>Department of Cell Biology, Wuxi School of Medicine, Jiangnan University, 1800 Lihu Dadao, Binhu District, Wuxi, Jiangsu 214122, P.R. China

Received: 20 January 2025 / Accepted: 4 March 2025

Published online: 15 March 2025

### References

1. Zhao B, Rehati P, Yang Z, Cai Z, Guo C, Li Y. The potential toxicity of microplastics on human health. *Sci Total Environ*. 2024;912:168946. <https://doi.org/10.1016/j.scitotenv.2023.168946>.
2. Allouzi MMA, Tang DYY, Chew KW, Rinklebe J, Bolan N, Allouzi SMA, et al. Micro (nano) plastic pollution: the ecological influence on soil-plant system and human health. *Sci Total Environ*. 2021;788:147815. <https://doi.org/10.1016/j.scitotenv.2021.147815>.
3. Cox KD, Covernton GA, Davies HL, Dower JF, Juanes F, Dudas SE. Human consumption of microplastics. *Environ Sci Technol*. 2019;53(12):7068–74. <http://doi.org/10.1021/acs.est.9b01517>.
4. Deng Y, Zhang Y, Lemos B, Ren H. Tissue accumulation of microplastics in mice and biomarker responses suggest widespread health risks of exposure. *Sci Rep*. 2017;7:46687. <https://doi.org/10.1038/srep46687>.
5. Senathirajah K, Attwood S, Bhagwat G, Carbery M, Wilson S, Palanisami T. Estimation of the mass of microplastics ingested - A pivotal first step towards human health risk assessment. *J Hazard Mater* 404(Pt B). 2021;124004. <https://doi.org/10.1016/j.jhazmat.2020.124004>.
6. Liu X, Zhao Y, Dou J, Hou Q, Cheng J, Jiang X. Bioeffects of inhaled nanoplastics on neurons and alteration of animal behaviors through deposition in the brain. *Nano Lett*. 2022;22(3):1091–9. <https://doi.org/10.1021/acs.nanolett.1c04184>.
7. Kopatz V, Wen K, Kovács T, Keimowitz AS, Pichler V, Widder J, et al. Micro- and Nanoplastics Breach the Blood-Brain Barrier (BBB): Biomolecular Corona's Role Revealed. *Nanomaterials* (Basel). 2023;13(8). <https://doi.org/10.3390/nano13081404>.
8. Kaur M, Sharma A, John P, Bhatnagar P. Manifestation of polystyrene microplastic accumulation in brain with emphasis on morphometric and histopathological changes in limbic areas of Swiss albino mice. *Neurotoxicology*. 2024;105:231–46. <https://doi.org/10.1016/j.neuro.2024.10.008>.
9. Lee CW, Hsu LF, Wu IL, Wang YL, Chen WC, Liu YJ, et al. Exposure to polystyrene microplastics impairs hippocampus-dependent learning and memory in mice. *J Hazard Mater*. 2022;430:128431. <https://doi.org/10.1016/j.jhazmat.2022.128431>.
10. Liu X, Yang H, Yan X, Xu S, Fan Y, Xu H, et al. Co-exposure of polystyrene microplastics and iron aggravates cognitive decline in aging mice via ferroptosis induction. *Ecotoxicol Environ Saf*. 2022;233:113342. <https://doi.org/10.1016/j.ecoenv.2022.113342>.
11. Liu C, She Y, Huang J, Liu Y, Li W, Zhang C, et al. HMGB1-NLRP3-P2X7R pathway participates in PM(2.5)-induced hippocampal neuron impairment by regulating microglia activation. *Ecotoxicol Environ Saf*. 2022;239:113664. <http://doi.org/10.1016/j.ecoenv.2022.113664>.
12. Dissing-Olesen L, LeDue JM, Rungta RL, Hefendehl JK, Choi HB, MacVicar BA. Activation of neuronal NMDA receptors triggers transient ATP-mediated microglial process outgrowth. *J Neurosci*. 2014;34(32):10511–27. <https://doi.org/10.1523/jneurosci.0405-14.2014>.
13. Sun Z, Zhan L, Liang L, Sui H, Zheng L, Sun X, et al. ZiBu PiYin recipe prevents diabetes-associated cognitive decline in rats: possible involvement of ameliorating mitochondrial dysfunction, insulin resistance pathway and histopathological changes. *BMC Complement Altern Med*. 2016;16:200. <https://doi.org/10.1186/s12906-016-1177-y>.
14. Choi GE, Lee HJ, Chae CW, Cho JH, Jung YH, Kim JS, et al. BNIP3L/NIX-mediated mitophagy protects against glucocorticoid-induced synapse defects. *Nat Commun*. 2021;12(1):487. <https://doi.org/10.1038/s41467-020-20679-y>.
15. Sun R, Liu M, Xiong F, Xu K, Huang J, Liu J, et al. Polystyrene micro- and nanoplastics induce gastric toxicity through ROS mediated oxidative stress and P62/Keap1/Nrf2 pathway. *Sci Total Environ*. 2024;912:169228. <https://doi.org/10.1016/j.scitotenv.2023.169228>.
16. Bean JC, Lin TW, Sathyamurthy A, Liu F, Yin DM, Xiong WC, et al. Genetic labeling reveals novel cellular targets of schizophrenia susceptibility gene: distribution of GABA and non-GABA ErbB4-positive cells in adult mouse brain. *J Neurosci*. 2014;34(40):13549–66. <https://doi.org/10.1523/jneurosci.2021-14.2014>.
17. Gao YZ, Wu XM, Zhou ZQ, Liu PM, Yang JJ, Ji MH. Dysfunction of NRG1/ErbB4 signaling in the Hippocampus might mediate Long-term memory decline after systemic inflammation. *Mol Neurobiol*. 2023;60(6):3210–26. <https://doi.org/10.1007/s12035-023-03278-y>.
18. Xu Y, Wang ML, Tao H, Geng C, Guo F, Hu B, et al. ErbB4 in parvalbumin-positive interneurons mediates proactive interference in olfactory associative reversal learning. *Neuropsychopharmacology*. 2022;47(7):1292–303. <https://doi.org/10.1038/s41386-021-01205-0>.
19. Schumacher MA, Hedl M, Abraham C, Bernard JK, Lozano PR, Hsieh JJ, et al. ErbB4 signaling stimulates pro-inflammatory macrophage apoptosis and limits colonic inflammation. *Cell Death Dis*. 2017;8(2):e2622. <https://doi.org/10.1038/cddis.2017.42>.
20. Krivosheya D, Tapia L, Levinson JN, Huang K, Kang Y, Hines R, et al. ErbB4-neuregulin signaling modulates synapse development and dendritic arborization through distinct mechanisms. *J Biol Chem*. 2008;283(47):32944–56. <https://doi.org/10.1074/jbc.M800073200>.
21. Mouton-Liger F, Dumurgier J, Cognat E, Hourregue C, Zetterberg H, Vanderstichele H, et al. CSF levels of the BACE1 substrate NRG1 correlate with cognition in Alzheimer's disease. *Alzheimers Res Ther*. 2020;12(1):88. <https://doi.org/10.1186/s13195-020-00655-w>.
22. Wang J, Huang J, Li YQ, Yao S, Wu CH, Wang Y, et al. Neuregulin 1/ErbB4 signaling contributes to the anti-epileptic effects of the ketogenic diet. *Cell Biosci*. 2021;11(1):29. <https://doi.org/10.1186/s13578-021-00536-1>.



23. Mao R, Hu M, Liu X, Ye L, Xu B, Sun M, et al. Impairments of GABAergic transmission in hippocampus mediate increased susceptibility of epilepsy in the early stage of Alzheimer's disease. *Cell Commun Signal*. 2024;22(1):147. <https://doi.org/10.1186/s12964-024-01528-7>.
24. Falls DL. Neuregulins: functions, forms, and signaling strategies. *Exp Cell Res*. 2003;284(1):14–30. [https://doi.org/10.1016/s0014-4827\(02\)00102-7](https://doi.org/10.1016/s0014-4827(02)00102-7).
25. Cools JMT, Goovaerts BK, Feyen E, Van den Bogaert S, Fu Y, Civati C, et al. Small-molecule-induced ERBB4 activation to treat heart failure. *Nat Commun*. 2025;16(1):576. <https://doi.org/10.1038/s41467-024-54908-5>.
26. Li Q, Ma Z, Qin S, Zhao WJ. Virtual Screening-Based drug development for the treatment of nervous system diseases. *Curr Neuropharmacol*. 2023;21(12):2447–64. <https://doi.org/10.2174/1570159x20666220830105350>.
27. Dao JJ, Zhang W, Liu C, Li Q, Qiao CM, Cui C, et al. Targeted ErbB4 receptor activation prevents D-Galactose-induced neuronal senescence via inhibiting ferroptosis pathway. *Front Pharmacol*. 2025;16. <https://doi.org/10.3389/fphar.2025.1528604>.
28. Prüst M, Meijer J, Westerink RHS. The plastic brain: neurotoxicity of micro- and nanoplastics. *Part Fibre Toxicol*. 2020;17(1):24. <https://doi.org/10.1186/s1298-9-020-00358-y>.
29. Oliveri Conti G, Ferrante M, Banni M, Favara C, Nicolosi I, Cristaldi A, et al. Micro- and nano-plastics in edible fruit and vegetables. The first diet risks assessment for the general population. *Environ Res*. 2020;187:109677. <https://doi.org/10.1016/j.envres.2020.109677>.
30. Zuccarello P, Ferrante M, Cristaldi A, Copat C, Grasso A, Sangregorio D, et al. Exposure to microplastics (< 10 µm) associated to plastic bottles mineral water consumption: the first quantitative study. *Water Res*. 2019;157:365–71. <https://doi.org/10.1016/j.watres.2019.03.091>.
31. Nair AB, Jacob S. A simple practice guide for dose conversion between animals and human. *J Basic Clin Pharm*. 2016;7(2):27–31. <https://doi.org/10.4103/0976-0105.177703>.
32. Shan S, Zhang Y, Zhao H, Zeng T, Zhao X. Polystyrene nanoplastics penetrate across the blood-brain barrier and induce activation of microglia in the brain of mice. *Chemosphere*. 2022;298:134261. <https://doi.org/10.1016/j.chemosphere.2022.134261>.
33. Qin X, Cao M, Peng T, Shan H, Lian W, Yu Y, et al. Features, potential invasion pathways, and reproductive health risks of microplastics detected in human uterus. *Environ Sci Technol*. 2024;58(24):10482–93. <https://doi.org/10.1021/acs.est.4c01541>.
34. Bai J, Wang Y, Deng S, Yang Y, Chen S, Wu Z. Microplastics caused embryonic growth retardation and placental dysfunction in pregnant mice by activating GRP78/IRE1α/JNK axis induced apoptosis and Endoplasmic reticulum stress. *Part Fibre Toxicol*. 2024;21(1):36. <https://doi.org/10.1186/s12989-024-00595-5>.
35. Deng Y, Chen H, Huang Y, Zhang Y, Ren H, Fang M, et al. Long-Term exposure to environmentally relevant doses of large polystyrene microplastics disturbs lipid homeostasis via bowel function interference. *Environ Sci Technol*. 2022;56(22):15805–17. <https://doi.org/10.1021/acs.est.1c07933>.
36. Campanale C, Massarelli C, Savino I, Locaputo V, Uricchio VFA. Detailed Review. Study on potential effects of microplastics and additives of concern on human health. *Int J Environ Res Public Health*. 2020;17(4). <https://doi.org/10.3390/ijerph17041212>.
37. Zhang T, Sun L, Wang T, Liu C, Zhang H, Zhang C, et al. Gestational exposure to PM(2.5) leads to cognitive dysfunction in mice offspring via promoting HMGB1-NLRP3 axis mediated hippocampal inflammation. *Ecotoxicol Environ Saf*. 2021;223:112617. <https://doi.org/10.1016/j.ecoenv.2021.112617>.
38. Wei S, Ma X, Chen Y, Wang J, Hu L, Liu Z, et al. Alzheimer's Disease-Derived outer membrane vesicles exacerbate cognitive dysfunction, modulate the gut microbiome, and increase neuroinflammation and Amyloid-β production. *Mol Neurobiol*. 2024. <https://doi.org/10.1007/s12035-024-04579-6>.
39. Liu C, Zhao Y, Zhao WJ. Positive effect of 6-Gingerol on functional plasticity of microglia in a rat model of LPS-induced depression. *J Neuroimmune Pharmacol*. 2024;19(1):20. <https://doi.org/10.1007/s11481-024-10123-z>.
40. Xiao Y, Fu H, Han X, Hu X, Gu H, Chen Y, et al. Role of synaptic structural plasticity in impairments of Spatial learning and memory induced by developmental lead exposure in Wistar rats. *PLoS ONE*. 2014;9(12):e115556. <https://doi.org/10.1371/journal.pone.0115556>.
41. Aliyev A, Chen SG, Seyidova D, Smith MA, Perry G, de la Torre J, et al. Mitochondria DNA deletions in atherosclerotic hypoperfused brain microvessels as a primary target for the development of Alzheimer's disease. *J Neurol Sci*. 2005;229–30. <https://doi.org/10.1016/j.jns.2004.11.040>. 285–92.
42. Flameng W, Borgers M, Daenen W, Stalpaert G. Ultrastructural and cytochemical correlates of myocardial protection by cardiac hypothermia in man. *J Thorac Cardiovasc Surg*. 1980;79(3):413–24.
43. Aliev G, Liu J, Shenk JC, Fischbach K, Pacheco GJ, Chen SG, et al. Neuronal mitochondrial amelioration by feeding acetyl-L-carnitine and lipoic acid to aged rats. *J Cell Mol Med*. 2009;13(2). <https://doi.org/10.1111/j.1582-4934.2008.00324.x>. 320–33.
44. Ozisik K, Yildirim E, Kaplan S, Solaroglu I, Sargon MF, Kilinc K. Ultrastructural changes of rat cardiac myocytes in a time-dependent manner after traumatic brain injury. *Am J Transpl*. 2004;4(6):900–4. <https://doi.org/10.1111/j.1600-6143.2004.00448.x>.
45. So YH, Shin HS, Lee SH, Moon HJ, Jang HJ, Lee EH, et al. Maternal exposure to polystyrene microplastics impairs social behavior in mouse offspring with a potential neurotoxicity. *Neurotoxicology*. 2023;99:206–16. <https://doi.org/10.1016/j.neuro.2023.10.013>.
46. Südhof TC. The cell biology of synapse formation. *J Cell Biol*. 2021;220(7). <https://doi.org/10.1083/jcb.202103052>.
47. Marinelli S, Basilio B, Marrone MC, Ragozzino D. Microglia-neuron crosstalk: signaling mechanism and control of synaptic transmission. *Semin Cell Dev Biol*. 2019;94:138–51. <https://doi.org/10.1016/j.semcdb.2019.05.017>.
48. Ryu J, Hong BH, Kim YJ, Yang EJ, Choi M, Kim H, et al. Neuregulin-1 attenuates cognitive function impairments in a Transgenic mouse model of Alzheimer's disease. *Cell Death Dis*. 2016;7(2):e2117. <https://doi.org/10.1038/cddis.2016.30>.
49. Calderón-Garcidueñas L, Mora-Tiscareño A, Melo-Sánchez G, Rodríguez-Díaz J, Torres-Jardón R, Styner M, et al. A critical proton MR spectroscopy marker of Alzheimer's disease early neurodegenerative change: low hippocampal NAA/Cr ratio impacts APOE ε4 Mexico City children and their parents. *J Alzheimers Dis*. 2015;48(4):1065–75. <https://doi.org/10.3233/jad-150415>.
50. Hokkanen SRK, Hunter S, Polvikoski TM, Keage HAD, Minett T, Matthews FE, et al. Hippocampal sclerosis, hippocampal neuron loss patterns and TDP-43 in the aged population. *Brain Pathol*. 2018;28(4):548–59. <https://doi.org/10.1111/bpa.12556>.
51. Wan J, Ma L, Jiao X, Dong W, Lin J, Qiu Y, et al. Impaired synaptic plasticity and decreased excitability of hippocampal glutamatergic neurons mediated by BDNF downregulation contribute to cognitive dysfunction in mice induced by repeated neonatal exposure to ketamine. *CNS Neurosci Ther*. 2024;30(2):e14604. <https://doi.org/10.1111/cns.14604>.
52. Mei L, Xiong WC. Neuregulin 1 in neural development, synaptic plasticity and schizophrenia. *Nat Rev Neurosci*. 2008;9(6). <https://doi.org/10.1038/nrn2392>. 437–52.
53. Min SS, An J, Lee JH, Seol GH, Im JH, Kim HS, et al. Neuregulin-1 prevents amyloid β-induced impairment of long-term potentiation in hippocampal slices via ErbB4. *Neurosci Lett*. 2011;505(1):6–9. <https://doi.org/10.1016/j.neulet.2011.05.246>.
54. Han S, Jeong YY, Sheshadri P, Su X, Cai Q. Mitophagy regulates integrity of mitochondria at synapses and is critical for synaptic maintenance. *EMBO Rep*. 2020;21(9):e49801. <https://doi.org/10.15252/embr.201949801>.
55. Reddy PH, Manczak M, Mao P, Calkins MJ, Reddy AP, Shirendeb U. Amyloid-beta and mitochondria in aging and Alzheimer's disease: implications for synaptic damage and cognitive decline. *J Alzheimers Dis*. 2010;2(Suppl 2):S499–512. <https://doi.org/10.3233/jad-2010-100504>.
56. Xu K, He Y, Moqbel SAA, Zhou X, Wu L, Bao J. SIRT3 ameliorates osteoarthritis via regulating chondrocyte autophagy and apoptosis through the PI3K/Akt/mTOR pathway. *Int J Biol Macromol*. 2021;175:351–60. <https://doi.org/10.1016/j.jbiomac.2021.02.029>.
57. Finley LW, Haas W, Desquiere-Dumas V, Wallace DC, Procaccio V, Gygi SP, et al. Succinate dehydrogenase is a direct target of Sirtuin 3 deacetylase activity. *PLoS ONE*. 2011;6(8):e23295. <https://doi.org/10.1371/journal.pone.0023295>.
58. Yang Y, Liu PY, Bao W, Chen SJ, Wu FS, Zhu PY. Hydrogen inhibits endometrial cancer growth via a ROS/NLRP3/caspase-1/GSDMD-mediated pyroptotic pathway. *BMC Cancer*. 2020;20(1):28. <https://doi.org/10.1186/s12885-019-6491-6>.
59. Wang Z, Meng S, Cao L, Chen Y, Zuo Z, Peng S. Critical role of NLRP3-caspase-1 pathway in age-dependent isoflurane-induced microglial inflammatory response and cognitive impairment. *J Neuroinflammation*. 2018;15(1):109. <https://doi.org/10.1186/s12974-018-1137-1>.
60. Penney J, Ralvenius WT, Loon A, Cerit O, Dileep V, Milo B, et al. iPSC-derived microglia carrying the TREM2 R47H/+ mutation are Proinflammatory and promote synapse loss. *Glia*. 2024;72(2):452–69. <https://doi.org/10.1002/glia.24485>.
61. Chaudhury AR, Gerecke KM, Wyss JM, Morgan DG, Gordon MN, Carroll SL. Neuregulin-1 and erbB4 immunoreactivity is associated with neuritic plaques in alzheimer disease brain and in a Transgenic model of alzheimer disease. *J*



- Neuropathol Exp Neurol. 2003;62(1):42–54. <https://doi.org/10.1093/jnen/62.1.42>.
62. Zhang Q, Xia W, Zhou X, Yang C, Lu Z, Wu S, et al. PS-MPs or their co-exposure with cadmium impair male reproductive function through the miR-199a-5p/HIF-1 $\alpha$ -mediated ferroptosis pathway. *Environ Pollut*. 2023;339:122723. <https://doi.org/10.1016/j.envpol.2023.122723>.
63. Jin H, Yang C, Jiang C, Li L, Pan M, Li D, et al. Evaluation of neurotoxicity in BALB/c mice following chronic exposure to polystyrene microplastics. *Environ Health Perspect*. 2022;130(10):107002. <https://doi.org/10.1289/ehp10255>.

### Publisher's note

Springer Nature remains neutral with regard to jurisdictional claims in published maps and institutional affiliations.